Zou *et al. Journal of Neuroinflammation* (2024) 21:215
https://doi.org/10.1186/s12974-024-03208-2

Journal of Neuroinflammation

RESEARCH Open Access

Microglia either promote or restrain TRAIL-mediated excitotoxicity caused by $A\beta_{1-42}$ oligomers

Jian Zou[1], Elizabeth McNair[1], Sagan DeCastro[1,4], Scott P. Lyons[3], Angie Mordant[3], Laura E. Herring[3], Ryan P. Vetreno[1,2] and Leon G. Coleman Jr[1,4*]

Abstract

Background Alzheimer's disease (AD) features progressive neurodegeneration and microglial activation that results in dementia and cognitive decline. The release of soluble amyloid (Aβ) oligomers into the extracellular space is an early feature of AD pathology. This can promote excitotoxicity and microglial activation. Microglia can adopt several activation states with various functional outcomes. Protective microglial activation states have been identified in response to Aβ plaque pathology in vivo. However, the role of microglia and immune mediators in neurotoxicity induced by soluble Aβ oligomers is unclear. Further, there remains a need to identify druggable molecular targets that promote protective microglial states to slow or prevent the progression of AD.

Methods Hippocampal entorhinal brain slice culture (HEBSC) was employed to study mechanisms of $A\beta_{1-42}$ oligomer-induced neurotoxicity as well as the role of microglia. The roles of glutamate hyperexcitation and immune signaling in Aβ-induced neurotoxicity were assessed using MK801 and neutralizing antibodies to the TNF-related apoptosis-inducing ligand (TRAIL) respectively. Microglial activation state was manipulated using Gi-hM4di designer receptor exclusively activated by designer drugs (DREADDs), microglial depletion with the colony-stimulating factor 1 receptor (CSF1R) antagonist PLX3397, and microglial repopulation (PLX3397 withdrawal). Proteomic changes were assessed by LC-MS/MS in microglia isolated from control, repopulated, or Aβ-treated HEBSCs.

Results Neurotoxicity induced by soluble $A\beta_{1-42}$ oligomers involves glutamatergic hyperexcitation caused by the proinflammatory mediator and death receptor ligand TRAIL. Microglia were found to have the ability to both promote and restrain Aβ-induced toxicity. Induction of microglial Gi-signaling with hM4di to prevent pro-inflammatory activation blunted Aβ neurotoxicity, while microglial depletion with CSF1R antagonism worsened neurotoxicity caused by Aβ as well as TRAIL. HEBSCs with repopulated microglia, however, showed a near complete resistance to Aβ-induced neurotoxicity. Comparison of microglial proteomes revealed that repopulated microglia have a baseline anti-inflammatory and trophic phenotype with a predicted pathway activation that is nearly opposite that of Aβ-exposed microglia. mTORC2 and IRF7 were identified as potential targets for intervention.

*Correspondence:
Leon G. Coleman Jr
leon_coleman@med.unc.edu

Full list of author information is available at the end of the article

Conclusion Microglia are key mediators of both protection and neurodegeneration in response to Aβ. Polarizing microglia toward a protective state could be used as a preventative strategy against Aβ-induced neurotoxicity.

Keywords Alzheimer's disease, Amyloid, Neurodegeneration, TRAIL, Microglia

Background

Alzheimer's disease (AD) is one of the most devastating neurological diseases with nearly 60 million people diagnosed worldwide [1]. The progression of AD pathology involves the accumulation and release of neurotoxic amyloid (Aβ) peptides into the extracellular space that peaks early in the disease process [2, 3]. These peptides are formed by processive proteolysis of amyloid precursor protein resulting in peptides of 38–42 amino acids in length [4]. Aβ oligomers can disrupt neuronal function by promoting neuronal hyperactivation [5], excitotoxic neuronal death [6–8], disrupting long-term potentiation [9, 10], and causing a loss of dendritic spines [11]. Neuronal hyperactivation in proximity to Aβ pathology is an early feature of AD that might contribute to cognitive dysfunction [12, 13]. Though Aβ plays a key role in AD pathogenesis, an ongoing mystery is that Aβ pathology is found in many cognitively normal aged individuals [14–16], with different patterns of tau spreading [17, 18]. Further, Aβ pathology only emerges with aging, even in most transgenic mouse models. Thus, it is likely that underlying factors in the neuro-environment that can change with age and vary across individuals determine the functional and pathological impacts of Aβ.

The neuroinflammatory state of individuals can vary greatly depending on genetic and environmental factors, as well as age, which could govern responses to Aβ. Indeed, neuroinflammation has been implicated in AD pathogenesis by human genetic and epidemiological studies [19–22]. Multiple preclinical studies have also found that inflammatory stimuli promote AD pathology [23–25]. Therefore, the status of the neuroimmune system might impact the resulting consequences of Aβ pathology. Further, there is a strong intersection between neurodegeneration and neuroinflammation, with several neurodegenerative processes being driven by immune mechanisms. At this intersection, the tumor necrosis factor-related apoptosis inducing ligand (TRAIL) is a key mediator of both neuronal death and neuroimmune signaling. Upon activation by TRAIL, death receptors 4 and 5 (DR4-5) promote FADD-mediated apoptosis or pro-inflammatory NF-kappaB activation [26]. TRAIL is increased in AD where it can promote both inflammation and Aβ-induced neuronal death [27–31]. However, it remains unclear how TRAIL facilitates Aβ-induced neurodegeneration, and how the consequences of Aβ can vary depending on the neuroimmune environment. We reported that TRAIL mediates neuronal death in response to proinflammatory Toll-like receptor activation, and that microglia play a key role in this response [32, 33]. Likewise, here we hypothesized that microglia play a key role in Aβ-induced neurotoxicity.

Microglia are key regulators of neuroinflammation and neurodegeneration in AD and with aging [34]. Microglial activation states are dynamic, with several populations found in healthy and disease states. In response to amyloid plaques, a subset of microglia adopt a phenotype that may be protective through increased phagocytosis [35–37]. However, responses to soluble Aβ oligomers can induce proinflammatory responses that may promote disease progression [8, 38–41]. For instance, Aβ can activate Toll-like receptor 4 (TLR4) signaling in microglia leading to proinflammatory activation [42–44]. Therefore, there are complex dynamics that can result in various populations of microglia with differing responses to various amyloid species. Further, the question remains as to why amyloid accumulation leads to AD pathology and neurodegeneration in some individuals, but not others. Microglial activation state can be regulated by multiple factors including cell surface receptors. Among these, G-protein coupled receptors (GPCRs) are critical for many of their effector functions [45]. For example, CX3CR1 is a Gi-coupled receptor in microglia that inhibits proinflammatory signaling. We and others have previously reported that induction of Gi signaling in microglia using designer receptors exclusively activated by designer drugs (DREADDs) can blunt microglial proinflammatory responses to exogenous stimuli [46–48]. Further, microglial responses are also impacted by their previous stimuli. This 'priming' or innate immune memory can be long lasting. However, we and others have reported that this microglial memory can also be 'erased' by microglial depletion and repopulation, resulting in a trophic/anti-inflammatory microglial phenotype [47, 49]. We investigated the roles of microglial activation state, using microglial Gi-inducing DREADDs (hM4di), and phenotype, using microglial repopulation. We found that pro-inflammatory microglia promote $A\beta_{1-42}$-induced neurotoxicity which involves TRAIL-mediated excitotoxicity. Microglia are key regulators, playing both protective and detrimental roles. Repopulated microglia (RM) were anti-inflammatory and neuro-protective, with repopulation prior to exposure to $A\beta_{1-42}$ preventing neuronal toxicity.

Methods

Reagents

Human $A\beta_{1-42}$ was purchased from Sigma-Aldrich (St Louis, USA). Recombinant mouse TRAIL protein was obtained from R&D. The CSF1R inhibitor PLX3397 was obtained from MedChemExpress (MCE, Monmouth Junction, USA).

Animals

Pregnant Sprague Dawley rat mothers were purchased from Charles River for brain slice culture (Raleigh, NC, USA). Male and female 5xFAD mice at 3 and 6 months of age were used for immunohistochemistry (N=7 male and 7 female at 3 mo and 8 male and 5 female at 6 mo, Jackson Laboratories, MMRRC Stock #034848-JAX). 5xFAD mice overexpress the mutant human amyloid beta (A4) precursor protein 695 (APP), the Swedish (K670N, M671L), Florida (I716V), and London (V717I) Familial Alzheimer's Disease (FAD) mutations, and the human PS1 harboring two FAD mutations (M146L, L286V). Animals were group-housed by sex in standard cages in a temperature- and humidity-controlled vivarium on a 12 h/12 h light/dark cycle and provided *ad libitum* access to food and water. This study was conducted in an AAALAC-accredited facility in strict accordance with NIH regulations for the care and use of animals in research. All experimental procedures were approved by the Institutional Animal Care and Use Committee at the University of North Carolina at Chapel Hill and conducted in accordance with NIH regulations (Protocol 24–040).

Hippocampal-entorhinal cortex brain slice culture (HEBSC)

The slice culture protocol followed in this study was approved by the Institutional Animal Care Use Committee of The University of North Carolina at Chapel Hill (Protocol 24–096) and was conducted in accordance with National Institute of Health regulations for the care and use of animals in research. Organotypic hippocampal-entorhinal cortical brain slice cultures (HEBSCs), which retain cellular architecture found in vivo, were prepared from early postnatal rat brain according to the techniques of Stoppini and colleagues (1991) with modifications as described previously (Zou and Crews, 2005; 2006). Cultures from postnatal donors are optimal as they show healthier cell morphology [50], survive for weeks in culture [47, 51], and undergo similar developmental maturation that is found in vivo such as functional maturation of synapses [52–55]. Briefly, rat neonates at postnatal day 7 were decapitated, the brain removed, and hippocampal-entorhinal complex dissected in Gey's buffer (Sigma-Aldrich, St. Louis, MO). Slices were transversely cut with McIlwain tissue chopper at a thickness of 375 µm and placed onto a 30 mm diameter membrane tissue insert, 10–13 slices/tissue insert. Slices were cultured with MEM containing 25 mM HEPES and Hank's salts, supplemented with 25% horse serum (HS)+5.5 g/L glucose+2 mM L-glutamine in a humidified 5% CO2 incubator at 36.5°C for 7 days in vitro (DIV), followed by 4DIV in MEM+12% HS, and then slices were cultured with MEM+6%HS. Serum-free N2-supplemented MEM was used to mix with MEM containing 25% HS throughout experiments.

Drug treatments and assessment of neurotoxicity

Mouse recombinant TRAIL was reconstituted in 0.1 M PBS and applied to slices at final concentration of 2ug/ml for 72 h in MEM+6%HS medium. For Aβ experiments, human $A\beta_{1-42}$ (Sigma) was reconstituted in an alkaline solution (1% NH_4OH) at concentration of 200µM followed by sonication according to the manufacturer's instructions and reports finding this increases activity [8]. To determine the cellular and molecular mechanisms underlying $A\beta_{1-42}$-induced neurotoxicity, we used 2–4µM for 72 h, which has previously been found to cause neuronal injury and death in cultured neurons and brain slice cultures (1–5µM) [6, 56]. Neurotoxicity was assessed using uptake of the fluorescent exclusion dye propidium iodide (PI). PI is a polar compound that is impermeable to a cell with an intact cell membrane but penetrates damaged cell membranes. Inside the cells, it binds nuclear DNA to generate the brightly red fluorescence. PI staining has been well characterized as accurately measuring neuronal degeneration in organotypic slice cultures by ourselves [32, 33, 57] and others using confirmatory approaches of neuronal death including lactate dehydrogenase release, Nissl cell staining, loss of neuronal MAP2, and Timm sulphide silver staining [58, 59]. Control sections typically have no detectable PI-fluorescence. PI (5 µg/ml) was added into the culture medium 24 h prior to the end of treatments and PI fluorescence images of individual slices were taken at the designated time points with an inverting Axiovert 100 microscopy and a KS 400 imaging software and analyzed with imaging program. Low magnification images were taken to allow visualization of the dentate gyrus and CA regions on each slice. The percentage of fluorescence-stained area was quantified using Fiji/ImageJ™. At least 9 slices per condition were assessed. Color-inverted representative images are displayed with fluorescence imaged as black for clear visualization as we have reported previously [32]. All images were taken with the same exposure to ensure accurate comparisons across groups.

Media glutamate measurement

Media was collected at the end of experiments as indicated and stored in -80°C until further analysis. The glutamate level in culture medium was determined by using

a glutamate ELISA kit obtained from Abnova (Walnut, CA). A total of 100μL medium was used for glutamate ELISA following the manufacturer's introduction.

Total RNA isolation, reverse transcription, and real time quantitative RT-PCR

For each specific experiment, the HEBSC slices were removed at the end of experiment, rinsed with cold PBS, followed by total RNA purification using miRNeasy Kit (Qiagen, CA). The total amount of RNA was quantified by nanodrop. For reverse transcription, either 200ng RNA from MV or 2 μg of RNA from slices was used to synthesize the first strand of cDNA using random primers (Invitrogen) and reverse transcriptase Moloney murine leukemia virus (Invitrogen). After a 1:2 dilution with water, 2 μl of the first strand cDNA solution was used for RT-PCR. The primer sequences for real time RT-PCR are shown in Table 1. SYBER Green Supermix (AB system, UK) was used as the RT-PCR solution. The real time RT-PCR was run with initial activation for 10 min at 95 °C and followed by 40 cycles of denaturation (95 °C, 40 s), annealing (58 °C, 45 s) and extension (72 °C, 40 s). The cycle threshold (CT) for each product was determined and normalized to internal standard β-actin or 18 S. Difference in CT values (ΔCT) was calculated [difference=2–(CT of target genes – CT of β-actin)=2–CT], and the result was expressed as the percentage compared to control.

Gi DREADD inhibition of proinflammatory microglia

Both control (pAAV.CMV.EGFP.WPRE) and Gi DREADD (pAAV.CD68.hM4Di.WPRE) vectors were obtained from VectorBuilder using the same construct that we and others have reported [46–48, 60]. This construct has been validated previously with co-immunofluorescence to induce hM4di expression specifically in microglia and not neurons or astrocytes [47, 60]. Briefly, HEBSC slices at 14DIV were transfected with AAV9.CD68.hM4Di (final multiplicity of transfection=1.16×10^9) for 24 h, followed by treatment with Clozapine-N-oxide (CNO) at concentration of 5 μM for 4 h, and then treated with trail or human beta-Amyloid for 72 h in MEM+6%HS medium. At the end of experiments, HEBSC slices were removed for further analysis and media were collected for ELISA measurements of glutamate.

Microglia depletion and repopulation

HEBSC slices at 4DIV were treated with the CSF1R inhibitor PLX3397 (1μM) for 7 days in regular culture medium (MEM containing 25% HS), followed by 3DIV in MEM+12% HS to deplete microglia. At the end of PLX3397 treatment, slices were either removed for immediate treatments (see below) or remained in PLX3397-free MEM+6%HS medium for 2 weeks to allow microglial repopulation as we have reported previously [47].

Immunomagnetic isolation of microglia (MACS)

The MACS isolation of microglia procedure was similar to methods reported previously [61]. Briefly, tissue was incubated for 45 min in a 37 °C water bath in 3 mL of enzyme digestion mix consisting of Hanks Balanced Salt Solution without magnesium or calcium (HBSS; ThermoFisher, Cat. #14175095), 5% fetal bovine serum (FBS; ThermoFisher, Cat. #A3160501), 10 μM HEPES (ThermoFisher, Cat. #15630080), 2.0 mg/mL collagenase A (Millipore, Cat. #10103586001), and 28 U/mL DNase I (Millipore, Cat. #10104159001). During incubation, samples were removed from the water bath every 15 min and passed through successively smaller glass Pasteur pipettes to gently dissociate tissue into a single cell suspension. Cell suspensions were filtered through MACS SmartStrainers (70 μm; Miltenyi Biotec, Cat. #130-098-462), centrifugated at 300×g at 4 °C for 10 min, supernatant aspirated, and pellets resuspended in 3.1 mL ice cold phosphate-buffered saline (PBS). Debris removal solution (900 μL; Miltenyi Biotec, Cat. #130-109-398) was added, samples centrifugated at 3,000×g at 4 °C for 10 min, debris removed by aspiration, and pellets resuspended with 90 μL of MACS buffer (1.0 mM EDTA and 1.0% bovine serum albumin in PBS, vacuum filtered). Samples were incubated with FcR blocking reagent (10 μL; Miltenyi Biotec, Cat. #130-092-575) for 10 min at 4 °C followed by incubation with 10 μL CD11b microbeads (Miltenyi Biotec, Cat. #130-105-634) at 4 °C for 15 min. Samples were washed with MACS buffer, centrifugated at 300×g at 4 °C for 10 min and resuspended with

Table 1 Primers for RT-PCR analyses

Genes	Forward (5′-3′)	Reverse (5′-3′)
TNFα	AGCCCTGGTATGAGCCCATGTA	CCGGACTCCGTGATGTCTAAG
Iba-1	GAGCTATGAGCCAGAGCAAG	CCCCAAGTTTCTCCAGCATT
TREM2	AAGCTTCTTACAGCCAGCAT	GTAGCAGAACAGAAGTCTTGGT
C1q	AGCTTTCTCAGCTATTCGGC	GGAGGAGGACACGATAGACA
P2RY12	GATTCTCACCAACAGGAGGC	ACAGAGTGTTCTCGGCATTG
Tmem119	AGTCGAACGGTCTAACAGGG	AAGAGGCTGAAGAACCCTCA
β-Actin	CTACAATGAGCTGCGTGTGGC	CAGGTCCAGACGCAGGATGGC

MACS buffer. Cells were then filtered through a nylon filter into magnetic bead columns (LS columns with the MidiMACS separator, Miltenyi Biotec), and CD11b positive and CD11b negative cell populations separated, and stored on ice. Samples were centrifugated at 300×g at 4 °C for 10 min, and washed 5 times in PBS to minimize the concentration of serum prior to LC-MS/MS.

LC-MS/MS proteomic analysis of isolated microglia

Sample Preparation. HEBSCs +/- microglial repopulation or $A\beta_{1-42}$ treatment (24 h) were isolated by MACS. Isolated microglia ($n=3$) were reduced with 5mM DTT at 37°C for 45 min. and alkylated with 15mM iodoacetamide at room temperature in the dark for 45 min. Samples were then diluted to 1 M urea with 50 mM ammonium bicarbonate and subjected to digestion with trypsin (Promega) overnight at 37°C at a 1:50 enzyme: protein ratio. Resulting peptides were acidified to 0.5% trifluoroacetic acid and desalted using ZipTips (Sigma). Eluates were dried via vacuum centrifugation, resuspended in 2% acetonitrile with 0.1% formic acid, and subjected to LC-MS/MS analysis.

LC-MS/MS. The peptide samples were analyzed by LC-MS/MS using an Easy nLC 1200 coupled to a QExactive HF mass spectrometer (Thermo Scientific). Samples were injected onto an Aurora Ultimate TS column (75 µm id × 25 cm, 1.7 µm particle size) (IonOpticks) and separated over a 90-minute period. The gradient for separation consisted of 5–45% mobile phase B at a 250 nl/min flow rate, where mobile phase A was 0.1% formic acid in water and mobile phase B consisted of 0.1% formic acid in 80% ACN. The QExactive HF was operated in data-dependent mode where the 15 most intense precursors were selected for subsequent fragmentation. Resolution for the precursor scan (m/z 350–1700) was set to 60,000, while MS/MS scans resolution was set to 15,000. The normalized collision energy was set to 27% for HCD. Peptide match was set to preferred, and precursors with unknown charge or a charge state of 1 and ≥7 were excluded.

LC-MS/MS Data analysis. Raw data files were searched against the Uniprot reviewed and unreviewed rat database (containing 47,932 entries, downloaded February 2024), appended with a contaminants database, using the Sequest HT search engine node within Proteome Discoverer (v3.1, Thermo Fisher). Enzyme specificity was set to trypsin, up to two missed cleavage sites were allowed, methionine oxidation and N-terminus acetylation were set as variable modifications and cysteine carbamidomethylation was set as a static modification. The Minora node was used to extract label-free quantification (LFQ) intensities. A 1% peptide-level false discovery rate (FDR) and a 1% protein-level FDR was used to filter all data. Match between runs was enabled, and a minimum of two peptides was required for label-free quantitation using the LFQ intensities. Perseus was used for further processing [62]. Proteins with >50% of missing values across the samples were filtered out. The remaining missing values were imputed from normal distribution within Perseus. Log_2 fold change (FC) ratios were calculated using the averaged Log_2 LFQ intensities of microglial repopulation or amyloid to control, and students t-test performed for each pairwise comparison, with p-values calculated. Proteins with p-values (<0.05) and $Log_2FC>0.5$ or $Log_2FC<-0.5$ were considered significant.

Statistical analysis

All statistics were performed using GraphPad Prism™ version 10.2.1. For preplanned orthogonal contrasts between two groups, unpaired two-tailed Student *t*-tests were employed. A $p<0.05$ was considered as significant. For comparisons with more than two multiple groups, 1-way or 2-way ANOVAs were used with Sidak's post-hoc testing when appropriate. Outliers were identified using Grubb's test (GraphPad).

Results

$A\beta_{1-42}$ causes glutamatergic excitotoxicity through induction of TRAIL

$A\beta_{1-42}$ caused robust increases in propidium iodide (PI) uptake in dentate gyrus and CA1 regions, consistent with neurotoxicity (Fig. 1A-B). As expected, control slices showed no measurable PI-labeled cell death consistent with our previous reports [32, 33, 63–65]. There was variability in the degree of neurotoxicity, which may be related to slight anatomical variations across slices. However, Aβ-induced toxicity was nearly completely abolished by the NMDA antagonist MK801. This Aβ-induced toxicity was associated with an increase in media glutamate levels that was also blocked by MK801 (Fig. 1C). Therefore, we assessed if glutamate causes release of TRAIL into culture media. Treatment of slices with glutamate (3mM) caused a rapid increase in levels of TRAIL in HEBSC tissue at 0.5 and 4 h, which is prior to detectable glutamate-induced neuronal death (Fig. 1D). At 24 h, when glutamatergic neurotoxicity is apparent, even higher increases in TRAIL were found. This indicates that $A\beta_{1-42}$-induced neurotoxicity involves glutamatergic hyperexcitability with activation of TRAIL and DR signaling.

Since $A\beta_{1-42}$ caused excitotoxicity and induced TRAIL, we next assessed the relationship between TRAIL and glutamate. HEBSC were treated with glutamate with or without αTRAIL antibodies for 24 h. Glutamate caused neuronal death in dentate gyrus and CA regions that was blocked by αTRAIL neutralizing antibodies (αTRAIL mAbs) in a concentration-dependent fashion (Fig. 2A-B). Likewise, treatment with TRAIL caused hippocampal

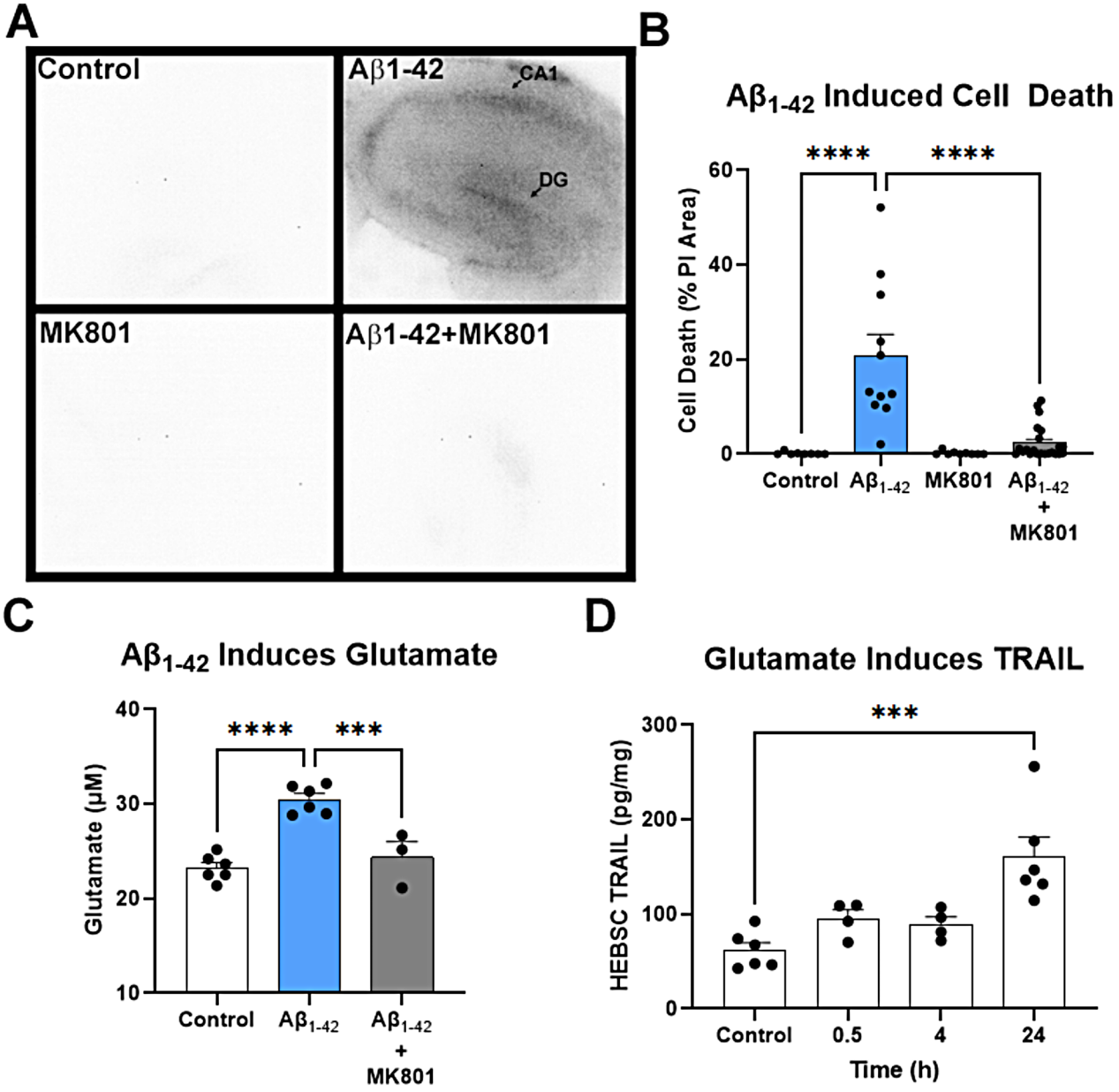

Fig. 1 Excitotoxic injury caused by $A\beta_{1-42}$ induces death receptor signaling. **(A)** Representative images of propidium iodide (PI) stain of HEBSCs treated with $A\beta_{1-42}$ (2μM)+/- MK801 (30μM). $A\beta_{1-42}$ increased PI uptake in dentate gyrus (DG) and CA regions. Images were converted to black and white images to improve visualization. **(B)** $A\beta_{1-42}$ increased PI-labeling by 18-fold, which was greatly blunted by MK801. Each data point represents an individual brain slice. $F_{3,54}$=21.5, $p < 0.0001$. ****$p < 0.0001$, Sidak's multiple comparison test. N=8 control, 11 $A\beta_{1-42}$, 9 MK801 alone, and 22 $A\beta_{1-42}$ + MK801 slices, 2 separate experiments. **(C)** $A\beta_{1-42}$ caused a ~ 50% increase in media glutamate measured by ELISA, which was blocked by MK801. MK801 alone (N=2) had no effect on media glutamate thus was combined with controls. Each data point is a measurement from an individual well. N=3–6/group $F_{2,13}$=21.2, ****$p < 0.0001$, Sidak's multiple comparison test. **(D)** Glutamate (3mM) caused a progressive increase in levels of TRAIL in HEBSC tissue above control (C) from 0.5 to 4 h (time points prior to detectable glutamate-induced cell injury), to 24 h when cytotoxicity is seen. N=4–6 per group, *q < 0.05, multiple *t*-tests versus control

neurotoxicity in a concentration-dependent manner that was prevented by MK801. Therefore, this indicates a feed-forward reciprocal relationship between glutamate and TRAIL, wherein a hyper-glutamatergic state induces TRAIL, which can then promote further excitotoxicity.

We next investigated the role of TRAIL in Aβ-induced neurotoxicity. First, we investigated if an association exists between TRAIL and Aβ in vivo. 5xFAD mice were assessed at two ages as pathology increases, 3 months and 6 months, in both males and females. Consistent

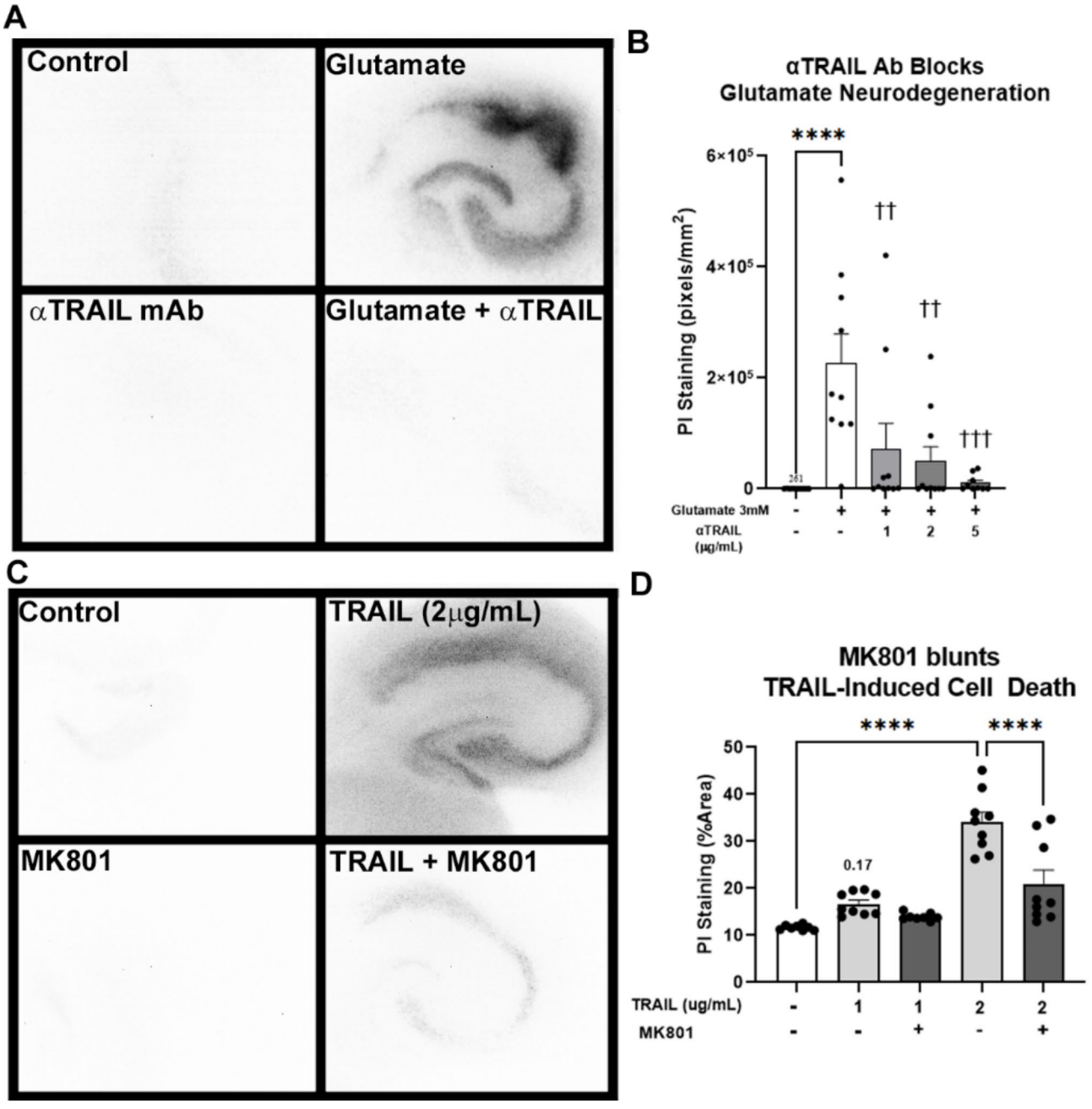

Fig. 2 A feed-forward reciprocal relationship between glutamate excitotoxicity and TRAIL. **(A)** Representative images of HEBSCs treated with glutamate (3mM) +/- αTRAIL monoclonal antibodies for 24 h. **(B)** Glutamate (3mM) caused robust increases in PI uptake in dentate gyrus and CA regions that was blocked by αTRAIL in a concentration-dependent manner. $F_{4,44}$=7.328, p=0.0001, ****p<0.0001 vs. control, ††p<0.01, †††p<0.001 vs. Glutamate 3mM+0 μg/mL αTRAIL, Sidak's multiple comparison test. N=9–10 slices/group **(C)** Representative images of HEBSCs treated with recombinant TRAIL +/- MK801. **(D)** TRAIL caused a concentration-dependent increase in neurotoxicity in dentate gyrus and CA regions that was prevented by MK801. F4,38=26.4, p<0.0001. ****p<0.0001, Sidak's multiple comparison test. N=8–10 slices/group

with previous reports, $A\beta_{1-42}$+plaque pathology was greater in females than males. As expected, in the subiculum, the number of $A\beta_{1-42}$+plaques increased from 3 to 6 months in both sexes (Fig. 3A-B). In females, TRAIL likewise increased from 3 to 6 months (Fig. 3C-D). Across both ages and all subjects, TRAIL and $A\beta_{1-42}$ plaque levels were positively correlated in the subiculum (Fig. 3E, R=0.42, *p<0.05). An age-related increase in Aβ was also seen in the dentate gyrus and CA1 (Supplemental Fig. 1). A similar correlation was observed in the dentate gyrus at 3 months (Fig. 3F), supporting an association between TRAIL expression and Aβ pathology. To determine directly if TRAIL mediates $A\beta_{1-42}$ excitotoxicity, we tested the impact of αTRAIL mAbs. We found

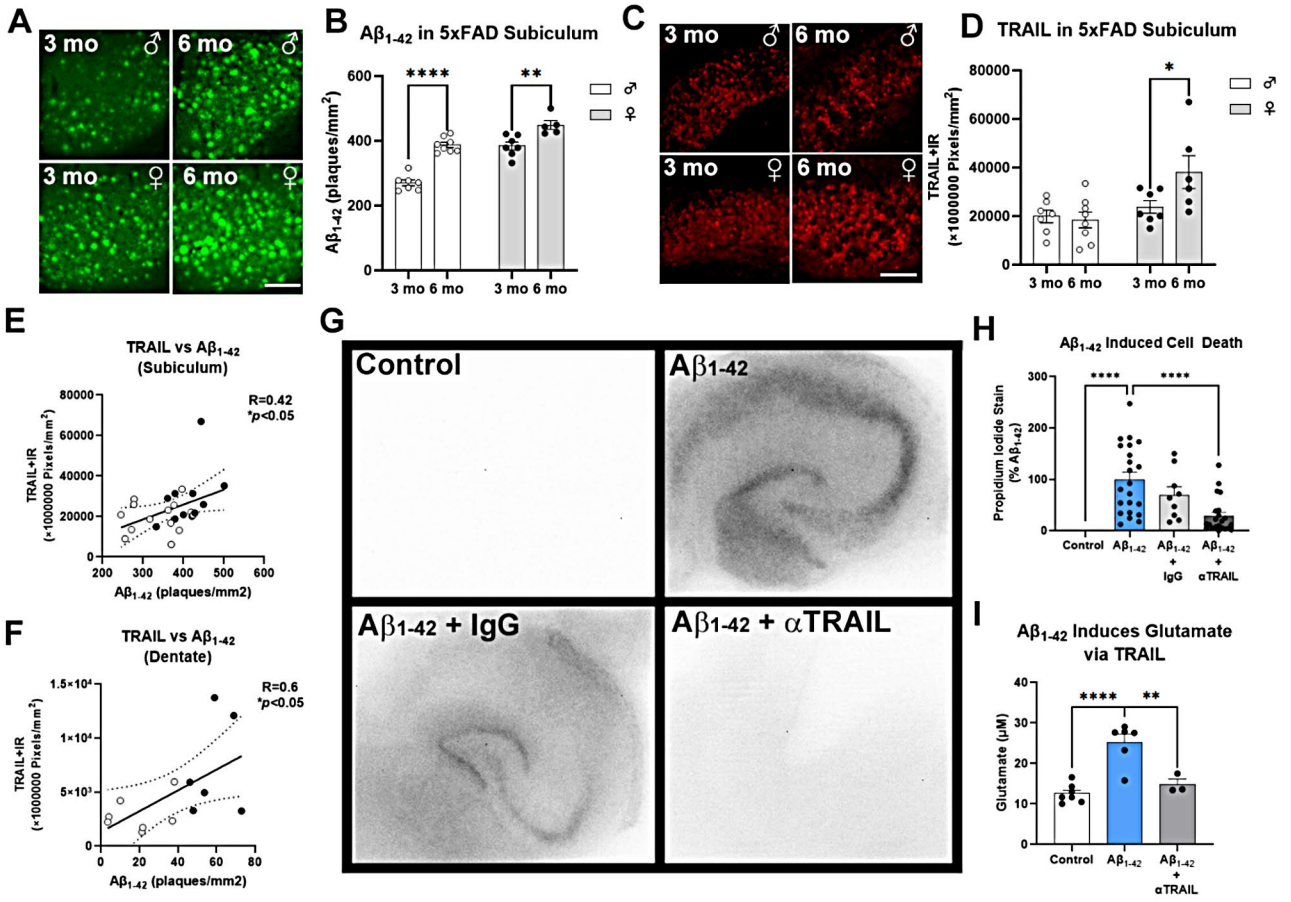

Fig. 3 TRAIL is associated with $A\beta_{1-42}$ in vivo, and mediates Aβ-induced neurotoxicity. **(A)** Images of $A\beta_{1-42}$ at 3 and 6 months in male and female subiculum. $N = 7$ male and 7 female at 3 mo. $N = 8$ male and 5 female at 6 mo. **(B)** $A\beta_{1-42}$ was increased in the subiculum with age in both sexes. Age effect: $F_{1,23} = 44.6$, $p < 0.0001$ **(C)** Images of TRAIL at 3 and 6 months in 5xFAD male and female subiculum. **(D)** Female 5xFAD mice showed an increase in TRAIL from 3 to 6 months. Sex effect: $F_{1,24} = 9.2$, $p < 0.01$, $^{**}p < 0.01$ Sidak's post-test. Scale bar 100 μm. **(E)** A positive correlation was seen between TRAIL and $A\beta_{1-42}$ across all subjects. $R = 0.42$, $^{*}p < 0.05$. **(F)** TRAIL and $A\beta_{1-42}$ showed a strong positive correlation at 3 months in dentate gyrus. $R = 0.6$, $^{*}p < 0.05$. **(G)** Images of HEBSCs treated with $A\beta_{1-42}$ +/- αTRAIL. **(H)** $A\beta_{1-42}$ caused robust neuronal injury that was blocked by αTRAIL but not isotype control antibodies. $F_{3,59} = 13.1$, $p < 0.0001$. $N = 10–22$ slices/group, 2 experiments combined. **(I)** $A\beta_{1-42}$ increases in media glutamate were blocked by αTRAIL antibodies. $F_{2,13} = 21.2$, $N = 3–7$ wells/group $p < 0.0001$. **, $p < 0.01$, $^{****}p < 0.0001$, Sidak's post-test

that αTRAIL mAbs blocked $A\beta_{1-42}$-induced neurotoxicity (Fig. 3G-H) and prevented Aβ-induced increases in media glutamate (Fig. 3I). Together, this supports that $A\beta_{1-42}$ induces the expression of TRAIL, which then promotes glutamatergic excitotoxicity.

Proinflammatory microglia promote Aβ-induced neurotoxicity

Microglia are key contributors to neurodegeneration and can facilitate TRAIL-mediated neurodegeneration in response to TLR signaling [32, 33]. Therefore, we hypothesized that proinflammatory microglia promote neuronal injury caused by $A\beta_{1-42}$. To specifically inhibit microglial proinflammatory activation in a biologically relevant manner, we expressed Gi designer receptor exclusively activated by designer drugs (DREADD) in microglia (AAV9.CD68.hM4di). We and others have previously used this approach and found this construct expresses Gi DREADDs specifically in microglia [47, 60], and blunts proinflammatory activation within microglia [46–48, 60, 66]. Addition of the DREADD ligand CNO results in stimulation of Gi signaling. In a subset of HEBSCs we confirmed that DREADD-mediated induction of Gi signaling in microglia with returned both TNFα and Iba-1 in the presence of $A\beta_{1-42}$-induced proinflammatory microglia activation in HEBSCs, increasing the expression of TNFα and Iba-1 (Supplemental Fig. 2A-B), with CNO alone having no effect. We then assessed the impact of microglial Gi activation on $A\beta_{1-42}$-induced excitotoxicity. $A\beta_{1-42}$ again caused robust PI labeling in hippocampal dentate gyrus and CA regions. Addition of an AAV9.EGFP control virus had no effect on $A\beta_{1-42}$-induced toxicity, neither did the AAV9.CD68.hM4di virus in the absence of CNO (Fig. 4A, top right panel). However, Gi

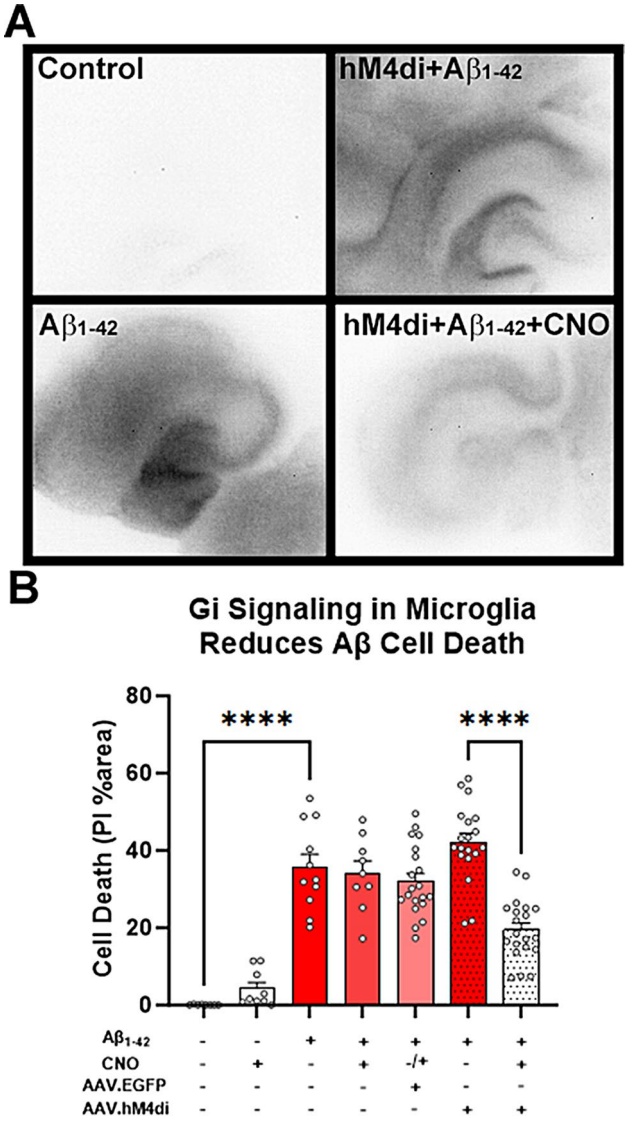

Fig. 4 Gi DREADD inhibition of microglia blunts Aβ-induced neurotoxicity. HEBSCs were treated with AAV.CD68.hM4di (DREADD) or AAV.EGFP control viruses for 24 h prior to treatment +/- $A\beta_{1-42}$ +/- the DREADD ligand CNO (5μM). **(A)** Representative images of HEBSC treated +/- $A\beta_{1-42}$ +/- Gi DREADD activation. **(B)** $A\beta_{1-42}$ caused robust hippocampal neurodegeneration that was blunted by microglial Gi DREADD activation by 54%. One-way ANOVA, $F_{7,88}$=33.7, $p < 0.0001$. *$p < 0.05$, **$p < 0.01$, **$p < 0.001$, ****$p < 0.0001$ Sidak's multiple comparisons test

DREADD activation by CNO caused a 54% reduction in $A\beta_{1-42}$ induced excitotoxicity (Fig. 4B). Thus, Gi inhibition of proinflammatory microglia can mitigate neuronal toxicity caused by $A\beta_{1-42}$.

Native resting and repopulated microglia (RM) restrain Aβ-induced neurotoxicity

Microglia adopt complex phenotypes both at rest and in response to insults. Since DREADD-mediated induction of Gi signaling in microglia blunted $A\beta_{1-42}$ toxicity, we hypothesized that microglia are required for this neuronal injury. To determine if microglia are required for Aβ-induced neurotoxicity, we used microglial depletion with the colony stimulating factor 1 receptor (CSF1R) antagonist PLX3397 (PLX). We have reported previously that this results in >90% depletion of microglia in HEBSCs [47, 67]. Microglial depletion alone did not cause any detectable changes in PI uptake (Fig. 5A, lower left panel). $A\beta_{1-42}$ again caused robust neuronal death, with some variability across sections likely due to slight anatomical differences as well as slight differences between the 2 repeated experiments. However, microglial depletion resulted in a 20% increase in neuronal injury caused by $A\beta_{1-42}$ (Fig. 5A-B). This indicates that resting microglia also play an important role in limiting Aβ-induced neurotoxicity. To determine if this was specific to amyloid, we next tested the impact of microglial depletion on cell death caused by TRAIL. A concentration of TRAIL was used that causes a moderate level of neuronal death (Fig. 5C, top right panel). Microglial depletion resulted in a profound 4-fold enhancement of TRAIL-induced cell death (Fig. 5D). Thus, microglia also play a key role in limiting neuronal death in the setting of Aβ and TRAIL-induced neurodegeneration.

The dichotomy between the impact of resting and proinflammatory microglia on neurodegeneration illustrates the complex and diverse phenotypes microglia adopt in response to insults. Though some resting microglia restrained neuronal injury to a degree, others promoted toxicity in response to Aβ. Therefore, polarization of all microglia to a protective phenotype could have therapeutic value. Microglial regeneration is an approach that has the potential to populate the brain with protective microglia [68, 69]. Therefore, we next investigated the impact of repopulated microglia (RM) on neuronal injury caused by amyloid. Microglia were first depleted using PLX3397, followed by removal of PLX for 14 days to allow microglial repopulation (Fig. 6A). As we reported previously [47], microglial depletion reduced expression of microglia-associated genes (*Iba-1*, *C1q*, and *Trem2*) that rebounded with repopulation (Fig. 6B). We then isolated microglia from HEBSCs using MACS for CD11b (Fig. 6C) which resulted in microglial enriched fractions (Fig. 6D). Consistent with our previous reports, RM adopted a protective phenotype, with nearly a 2-fold increase in BDNF compared to native microglia (Fig. 6E). Therefore, we next assessed if Aβ-induced neurotoxicity is different in brain slices with naïve versus repopulated microglia. In slices with native microglia, $A\beta_{1-42}$ caused robust PI uptake in the hippocampal dentate gyrus and CA regions above (Fig. 6F, top panel). However, in brain slices with RM, virtually no neuronal injury was found in response to $A\beta_{1-42}$ (Fig. 6F-G). This illustrates a key role of microglia in Aβ-neurotoxicity and the protective ability of modulating microglial phenotype.

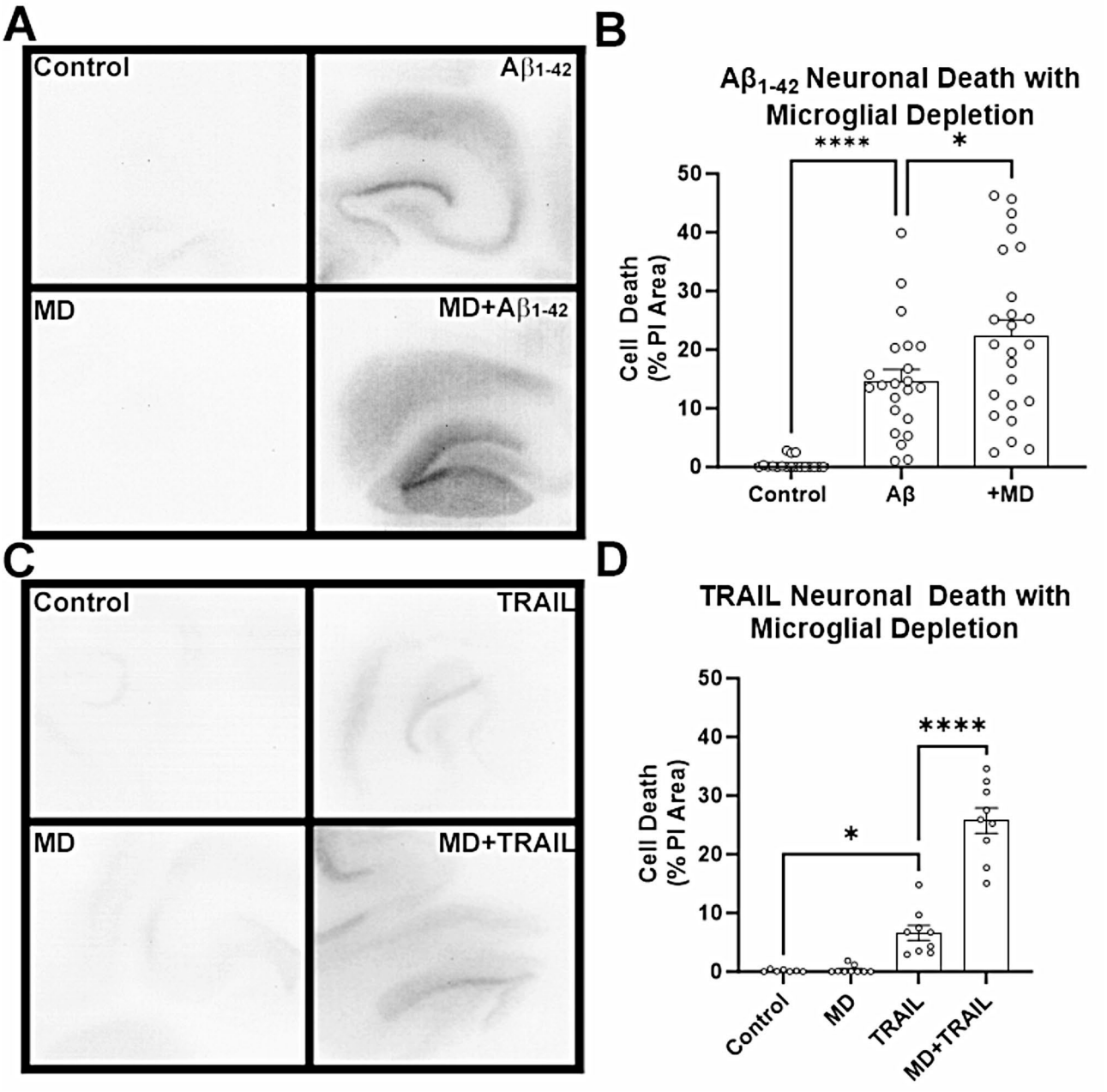

Fig. 5 Naïve microglia restrain neurotoxicity caused by Aβ and TRAIL. **(A)** Representative images of control or microglia depleted (MD) HEBSCs treated +/- $Aβ_{1–42}$. **(B)** $Aβ_{1–42}$ caused significant increases in PI uptake in the dentate gyrus and CA regions that was ~20% greater in MD slices. $F_{2,61}$=24.0, $p < 0.0001$. *$p < 0.05$, ****$p < 0.001$, Sidak's multiple comparisons test. N=18–24 slices/group, 2 separate experiments combined. Each data point represents an individual brain slice. **(C)** Representative images of control or MD HEBSCS +/- TRAIL (500 ng/mL). **(D)** TRAIL (500ng/mL) caused a moderate amount of neuronal injury that was enhanced by nearly 4-fold in the absence of microglia. $F_{5,45}$=52.2, $p < 0.0001$. *$p < 0.05$, ****$p < 0.001$, Sidak's multiple comparisons test. N=7–9 slices/group

Differential proteomes in repopulated versus naïve microglia

Since HEBSCs with RM showed resistance to neuronal injury caused by $Aβ_{1–42}$, we assessed differences in the proteome of RM to identify potential therapeutic targets. After treatment, microglia were isolated by MACS and assessed by LC-MS/MS. We measured 3065 proteins with a strong enrichment of previously identified microglial-enriched proteins [70] Tmsb4x, Ctsd, Psap, Ctsb, AIF1, Pkn3, Hexb, Itgam, and CD68, which were orders of magnitude higher than GFAP (Supplemental Fig. 3A). In RM vs. control microglia, 130 differentially expressed proteins were found, with RM showing mostly reductions in protein levels (Fig. 7A). Consistent with our

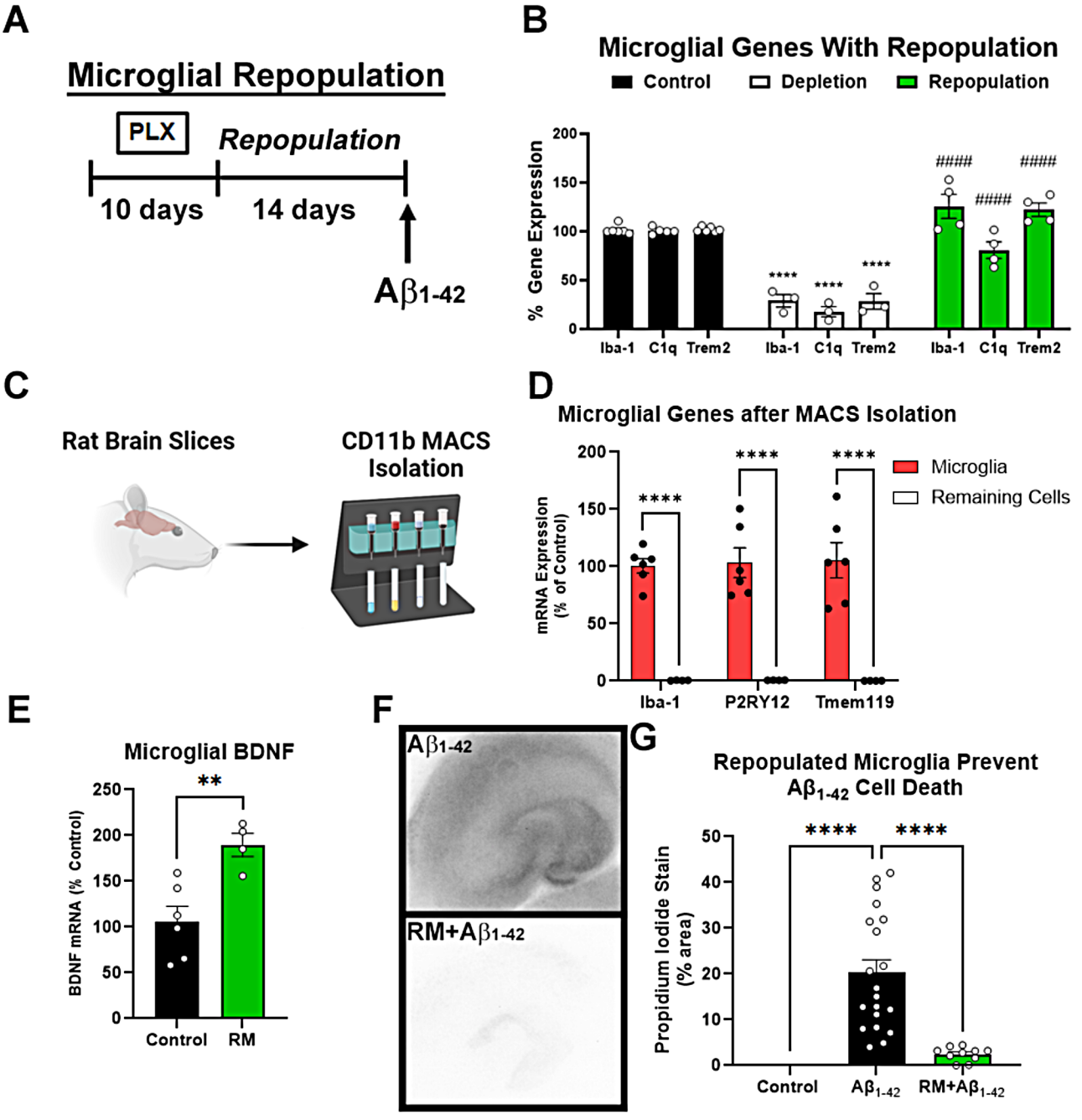

Fig. 6 Microglial repopulation strongly reduces Aβ-induced neurotoxicity. **(A)** Experimental design for microglial repopulation in brain slice culture. **(B)** Expression of microglial genes at baseline, after depletion and after repopulation. Each data point represents the average of two technical replicates from different culture wells. 2-way ANOVA. $F_{3,34}$=7.4, p = 0.0006. Tukey's multiple comparisons test. ****p < 0.0001 Control vs. Depletion, ####p < 0.0001, Depletion vs. Repopulation. N = 3–6/group. **(C)** Depiction of microglial isolation by CD11b + MACS. **(D)** Expression of microglial genes after MACS isolation in the microglial fraction and the remaining cells. 2-way ANOVA, $F_{2,24}$=136.9, p < 0.00001****p < 0.0001 Sidak's post-test. **(E)** Microglia were isolated from HEBSCs containing either native or RM by MACS. RM showed increased expression of BDNF compared to native microglia. **(F)** Represented image of PI staining in HEBSCs with either naïve or RM treated with $A\beta_{1-42}$ (1μM) for 4 days. **(G)** Quantification of robust increases in neurotoxicity after $A\beta_{1-42}$ treatment in HEBSCs with naïve, but not repopulated microglia. 1-way ANOVA, $F_{2,37}$=21.72, p < 0.0001. N = 10–20 slices/group

previous findings [47], ingenuity pathway analysis (IPA) predicted that RM have a less pro-inflammatory phenotype (Fig. 7B). Interferon (IFN) signaling was particularly impacted, with Interferon Regulatory Factor 5 (IRF5), IRF7, IFNA2, RIG-I, and IFNL1 predicted to be reduced along with IL-6 and colony-stimulating factor 1 (CSF1). Activity of RICTOR, however, which inhibits IL-6 was predicted to be increased. Several other pathways were

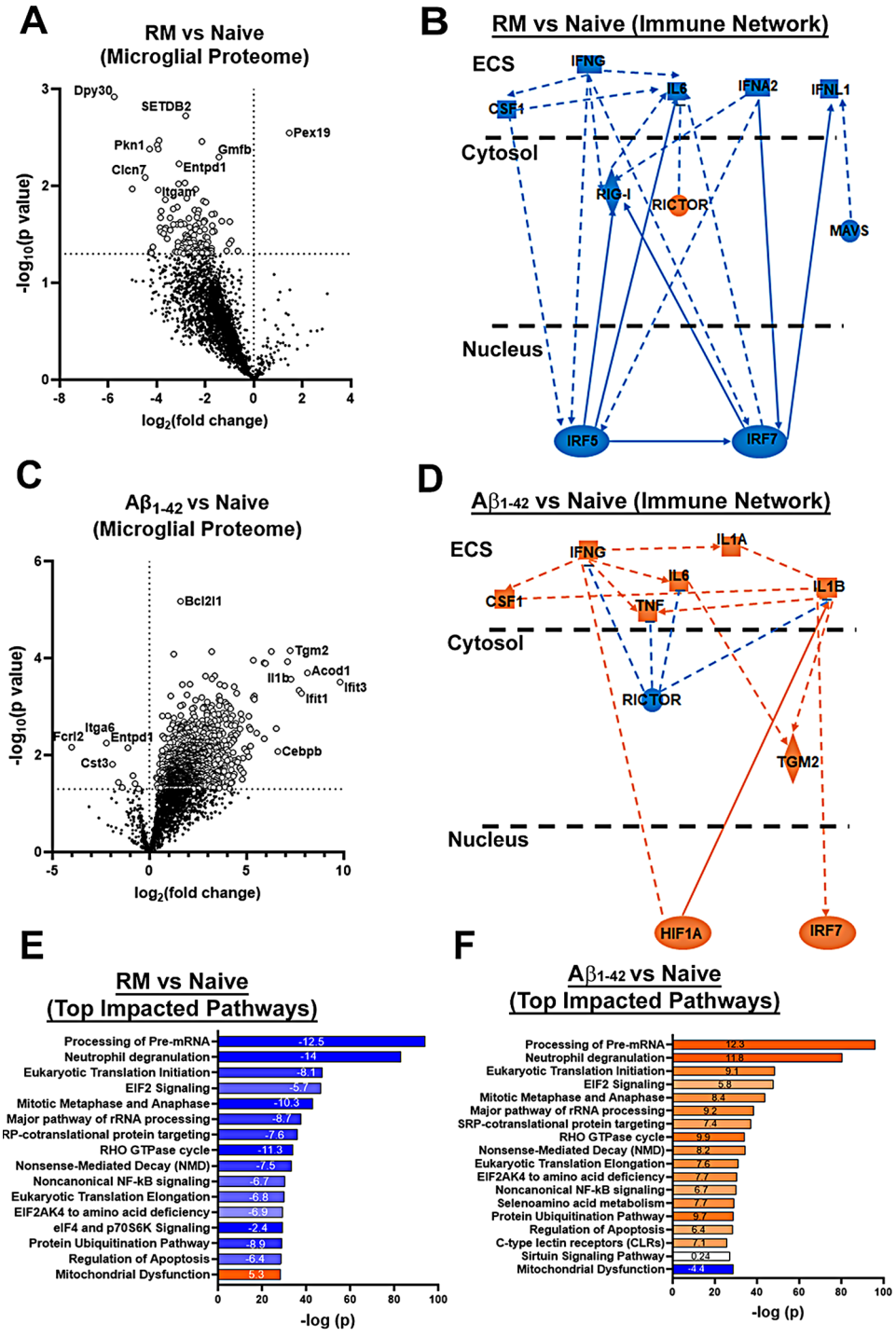

Fig. 7 Repopulated microglia (RM) feature an anti-inflammatory baseline that informs neuroprotective treatment strategies. **(A-B)** HEBSCs underwent microglial depletion with the CSFR1 antagonist PLX3397, with repopulation by removal of the compound. Microglia were isolated by MACS and their proteomes assessed by LC-MS/MS. **(A)** RM showed reduction of several proteins compared to naïve microglia. **(B)** Ingenuity pathway analysis (IPA) predicted downregulation of multiple proinflammatory gene pathways in RM. ECS-extracellular space. **(C-D)** HEBSCs were treated +/- $A\beta_{1-42}$ for 24 h followed by MACS microglial isolation and LC-MS/MS proteomics. **(C)** Microglia from $A\beta_{1-42}$-treated HEBSCs showed increased expression of several proteins. **(D)** IPA predicted activation of several pro-inflammatory pathways in naïve microglia from HEBSCs treated with $A\beta_{1-42}$. **(E)** IPA canonical pathways predicted to be altered in RM. **(F)** IPA canonical pathways predicted to be altered in microglia from HEBSCs treated with $A\beta_{1-42}$. $N = 3$ culture wells/group

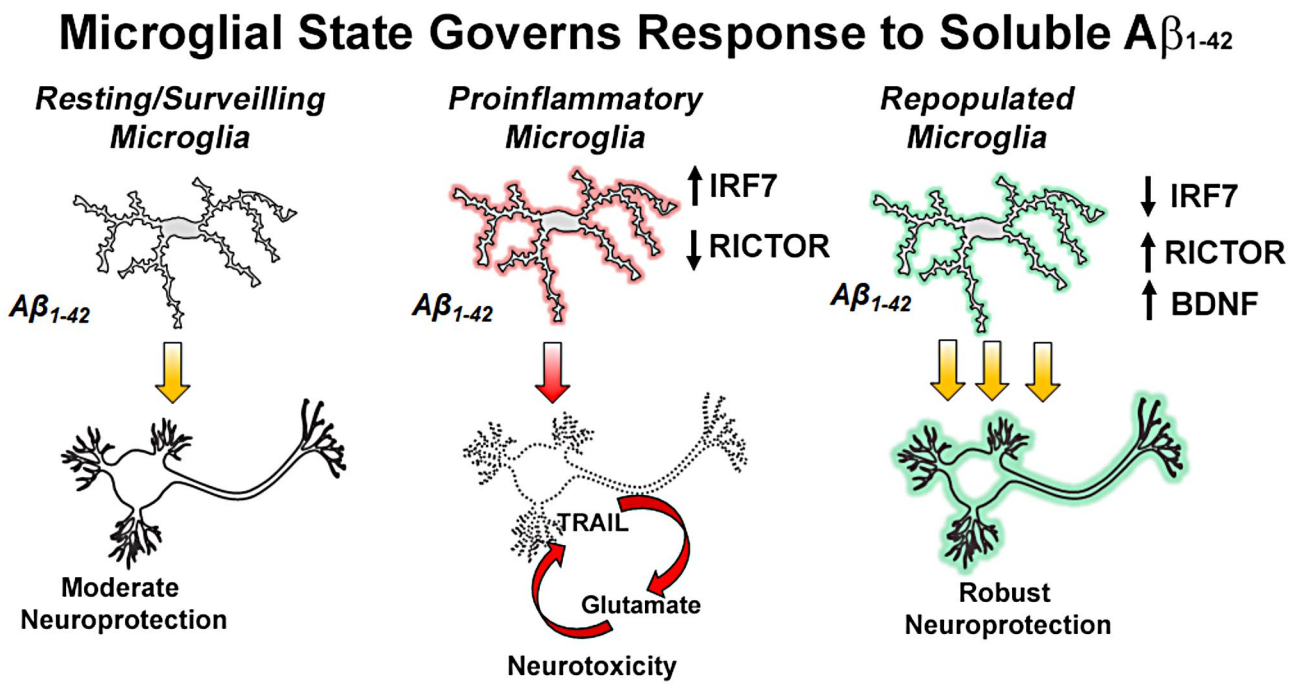

Fig. 8 Summary of findings. Microglial intrinsic state determines the impact of soluble $A\beta_{1-42}$ on neurons. Resting/surveilling microglia exert modest protection, as microglial depletion slightly increases neuronal death. Proinflammatory microglia have increased IRF7 and reduced RICTOR signaling, and promote neuronal death mediated by TRAIL-induced excitotoxicity. Repopulated microglia have reduced IRF7 signaling with increased RICTOR activation and BDNF levels, and result in robust neuroprotection when exposed to soluble $A\beta_{1-42}$

also predicted to be reduced including lipid metabolic pathways (Supplemental Fig. 3B). We then assessed the proteome of microglia isolated from HESCSs after $A\beta_{1-42}$ treatment for 24 h. Twenty-four hours was chosen to prevent confounding factors caused by cell injury, which we see in our model at 4 days of treatment, but not 24 h. $A\beta_{1-42}$ caused a robust alteration in the microglial proteome with 1249 proteins altered, and 1240 of these being increased (Fig. 7C). Importantly, we found a high level of agreement with a previous proteomic assessment of microglia isolated in vivo from 3 to 6-month-old APP-PS1 mice [70], which feature Aβ pathology (Supplemental Fig. 3C). Interestingly, we found several immune pathways were predicted to be in the opposite direction as found in RM (Fig. 7D, Supplemental Fig. 3D). For instance, IFNγ, IL-6, IRF7, IL-1β, and CSF1 were predicted to be increased, with RICTOR signaling predicted to be reduced. Further, canonical pathways associated with transcription, translation, and apoptosis were predicted to be reduced in RM (Fig. 7E), while they were increased with $A\beta_{1-42}$ treatment (Fig. 7F). Expression of mitochondrial components, however, (termed the mitochondrial dysfunction pathway by IPA) were increased in RM and reduced with $A\beta_{1-42}$.

Discussion

Amyloid accumulation is one of the earlier known events in the pathogenesis of AD. Accumulation of extracellular amyloid promotes secondary tau pathology and neurodegeneration. However, soluble Aβ oligomers such as $A\beta_{1-42}$ have been found to be neurotoxic [5, 6, 9–11], with speculation that inflammatory activation downstream of Aβ promotes subsequent toxicity [2]. A role for Aβ-induced excitotoxicity has been described [6], as well as a role for TRAIL [28, 30]. However, the interplay between excitation and TRAIL, and the role of microglia, had not been fully defined. Further, it has been unknown why cerebral amyloid accumulation occurs without clear sequalae in many cognitively normal aged individuals. Here, we find TRAIL directly mediates Aβ-induced excitotoxicity in a feed-forward manner, with microglial intrinsic state being a key governing factor that determines the downstream consequences of Aβ, resulting either by promoting or restraining neurodegeneration (Fig. 8).

TRAIL is a mediator of both cell death and inflammation [26, 27, 71]. Therefore, it could act directly on neurons to promote neuronal injury or through a glial intermediary. Several years ago, increased levels of TRAIL were found in AD brain in proximity to plaques [29], and neutralizing antibodies targeting TRAIL or its receptor DR5 were found to prevent Aβ-induced cell death in SH-SY5Y and primary mouse neurons [28,

30]. Systemic administration of an anti-TRAIL antibody subsequently was found to improve learning and memory function and reduce proinflammatory activation in 3xTg-AD mice [72], though these benefits may be due to the tempering of peripheral immune responses [73]. Using HEBSCs, we confirmed that TRAIL neutralization directly inhibits neurotoxicity caused by $A\beta_{1-42}$ in brain tissue. Further, we found that TRAIL plays a fundamental and bi-directional role in excitotoxicity at large. TRAIL neutralization prevented glutamate-induced neuronal death in a concentration-dependent fashion, and TRAIL-induced neuronal death was blunted by MK801. This suggests a feed-forward mechanism, whereby TRAIL release in response to Aβ or other insults (e.g., stroke [74] or seizure) promotes neuronal injury through both direct (i.e. TRAIL/DR signaling) and indirect (enhanced glutamate release) mechanisms (Fig. 7). Neuronal hyperexcitability is a key early feature in AD pathology. Thus, TRAIL might promote neuronal circuit disruption through this pathway in vivo even in the absence of robust cell death. Interestingly, microglia were found to play a key role in TRAIL-induced neuronal death. HEBSC lacking microglia showed increased neuronal injury when treated with TRAIL, supporting a protective role of mature microglia. It is unclear if this is a direct action on microglial TRAIL receptors or a less specific, protective role of resting microglia. Our findings with $A\beta_{1-42}$, however, suggest the latter.

TRAIL is a member of the TNF superfamily which includes 19 known ligands and 29 receptors [75]. These ligands are type II transmembrane proteins that upon cleavage act as cytokine-like molecules. These ligands regulate immune activation across a variety of cell types, and a few such as FasL, TL1A and TRAIL can cause cell death in susceptible cell types [75, 76]. The consequence of this signaling is related to both ligand receptor expressed on responding cell types (e.g., death receptor vs. decoy receptor expression) as well as the nature of downstream signaling events (e.g., c-FLIP or caspase-8 coupling) [26, 77]. In the healthy adult brain receptors for TL1A, FasL, and TRAIL are typically expressed at low levels [78, 79]. However, upon injury or stress TRAIL death receptor expression increases, permitting TRAIL-mediated inflammation or cytotoxicity [32, 80, 81]. Thus, TRAIL death receptors may represent a promising pharmacological target against neurodegeneration. Multiple efforts have been made over the years to activate TRAIL signaling to treat cancer, using recombinant TRAIL or monoclonal antibodies that activate TRAIL receptors [82, 83]. However, this work and that of others cited herein, suggest that compounds that antagonize the TRAIL receptor could be of benefit in AD [27, 28], multiple sclerosis [84], or other neurodegenerative disorders featuring excitotoxicity, such as seizure or stroke [74, 81].

Our studies in vitro implicate a role for TRAIL and microglia in the acute reaction to Aβ oligomers, however additional findings also suggest a role in chronic AD pathology. In the 5xFAD, we found that TRAIL and Aβ were positively correlated in the dentate gyrus (at 3 months of age) as well as the subiculum (3 and 6 months of age), consistent with increases in TRAIL found in the human AD and AD mouse models [29, 31, 73, 85]. Others have found that neuronal loss occurs at later ages in the 5xFAD (9 months) with caspase activation beginning around 4 months of age, suggesting a role for apoptosis [86]. Since TRAIL can promote neuronal apoptosis, it would be of value in future work to determine if TRAIL inhibition prevents neuronal loss in the 5xFAD. In elderly individuals with memory concerns, circulating levels of TRAIL were positively correlated with loss of episodic and working memory [87]. Recently, the expression of the TRAIL receptor DR5 was found to be increased in the hypothalamus with aging, though TRAIL mRNA was reduced [88]. Other whole brain transcriptomic studies have not found differences in TRAIL gene expression with aging [89, 90], though TRAIL protein levels are increased in the AD brain. This suggests that Aβ, rather than aging itself may promote increases in TRAIL protein seen in AD.

Microglia are known to play complex roles in AD and other neurodegenerative diseases. Indeed, the role of microglia in AD is related to the stage of the disease as well as the proximity of microglia to disease pathology. First, microglia may play a role in the initiation of disease pathology. Many of the known AD risk alleles are associated with microglia, suggesting they may play a causative role in the disease [91–93]. Consistent with this idea, proinflammatory stimuli throughout the lifespan, have been found to promote both intraneuronal Aβ and tau pathology [23–25]. Thus, aberrant activation microglia through environmental exposures or genetic risk may promote the onset of AD pathology. As the disease progresses, microglia can continue to play a detrimental role. Soluble Aβ oligomers, which may be released early in disease progression and/or through diffusion, can induce microglial proinflammatory responses in through TLR4 [8, 38, 39, 42–44, 94]. TLR4-activated microglia promote neuronal death or injury, either directly [33, 95, 96] or through activation of astrocyte intermediates [97]. Thus, future studies should determine if reactive astrocytes participate in TRAIL-mediated neuronal death caused by Aβ. A recent study found that conditioned media from microglia treated with Aβ oligomers was neurotoxic consistent with our findings [98]. However, the work presented here reveals an important caveat, that the intrinsic microglial state prior to oligomeric Aβ exposure determines the consequences directed toward neurons, as was seen with the prevention of neuronal

death with repopulated microglia. Microglia also promote the formation of Aβ plaques [99], and subsequently contribute to synapse loss in AD through complement-mediated removal [100]. Proinflammatory microglia signaling later in the disease can promote tau pathology as well as Aβ-induced cell death [101, 102]. It is unclear if TRAIL modulates microglial activation to promote these pathologic features as well neuronal death, though this is an ongoing area of study. Together, this illustrates that microglia can play detrimental roles in AD pathology. Our findings are consistent with this, as inhibition of Gi-signaling in microglia, which inhibits proinflammatory activation, blunted Aβ-induced cell death. DREADD-induced Gi signaling in microglia has been found to be anti-inflammatory, blunting pro-inflammatory gene induction and pathology in pain and addiction models [47, 48, 60, 103]. Further, in vivo naturally occurring microglial inhibitory receptors, such as CX3CR1 are Gi-coupled [45]. The mechanism underlying this protection by microglial Gi-induction is not entirely clear and is a focus of future studies. However, Gi-coupled GPCRs such as CX3CR1, P2Y12, and P2Y13 are downregulated in phagocytic and seemingly protective disease-associated microglia [35]. Therefore, targeted induction of Gi signaling in microglia using small molecule agonists may be a promising future therapeutic approach.

Microglia also play protective roles in AD. We found that microglia depletion with CSFR1 antagonism worsened Aβ-induced neuronal injury consistent with a report using clodronate-depletion [104]. Other studies have elucidated mechanisms involving TREM2 and SYK that underlie the phagocytic roles for microglia that are in proximity to Aβ plaques [35–37]. Thus, there are apparent differences in the nature of microglial activation and its consequences toward neurons depending on the form of amyloid, whether soluble or in plaques, to which they are exposed. Beyond phagocytosis, microglia play many roles that may be involved in this protection. For instance, we and others recently reported that microglia release trophic extracellular vesicles that promote neurogenesis [46, 105], though upon proinflammatory activation the vesicular content changes and becomes neurotoxic [33, 46]. Whether microglial secretion of trophic extracellular vesicles underlies the observed protection is an ongoing area of study in our group.

Perhaps more striking than the protection associated with induction of Gi signaling in microglia was the protection against Aβ toxicity seen with microglial repopulation. Proteomic analysis of RM and $A\beta_{1-42}$ treatment revealed multiple potential therapeutic targets. These can be identified as molecules or pathways with opposite directional changes between RM and microglia from $A\beta_{1-42}$ treated slices. For instance, RM show a baseline anti-inflammatory state with lower levels of IFN signaling than control microglia, while $A\beta_{1-42}$ induced IFN signaling. TRAIL is an IFN-induced gene [106–109], and IFN signaling increases in microglia with age, as well as in rodent AD models and human AD brain [110–114]. A recent study on human AD brain found a unique microglial cluster enriched in differentially expressed AD risk genes shows a strong IFN signature and lysosomal dysfunction, with IRF7 being one of the top predicted regulatory transcription factors in this population [114]. In RM, IPA predicted a reduction in IRF7 signaling as opposed to an increase predicted with $A\beta_{1-42}$ exposure. IRF7 inhibition has been found to prevent deleterious innate immune responses in other settings [115] and could be beneficial in AD. IRF7 is downstream of TLR7, which has been found to cause neuronal death through caspase activation [33, 116, 117]. TLR7 antagonists are commercially available and were recently in clinical trials for the treatment of COVID-19 [118]. Brain penetrant versions of this compound exist, which we reported prevent TLR7/IRF7/TRAIL-mediated neuronal death in the setting of heavy alcohol use [32]. Therefore, it is necessary to test the efficacy of these compounds for the prevention of AD pathology. Other pathways were also oppositely regulated between RM and $A\beta_{1-42}$-exposed microglia, suggesting they may have efficacy in the prevention of Aβ-induced pathology. This includes RICTOR, CD40, and mitochondrial function. RICTOR is a component of the mTORC2 complex that declines with aging [119]. Microglial mTOR activation through RAPTOR (mTORC1) has been reported to reduce Aβ pathology in 5xFAD mice [120]. Our findings suggest that mTORC2 agonists could also be protective. CD40 signaling impairs microglial phagocytosis of Aβ [121], and was reduced in RM. Therefore, CD40 antagonists could also be of benefit as they may promote Aβ phagocytosis and reduce the negative consequences of microglial proinflammatory activation. Further, mitochondrial metabolism was oppositely activated between RM and $A\beta_{1-42}$-microglia. This suggests that oxidative phosphorylation might differ between RM and $A\beta_{1-42}$-microglia, which is an area of ongoing study. Opposing activation of AD-associated pathways in RM may underly their protection. Consistent with these findings, a recent study found that microglial repopulation in 5xFAD mice improves cognitive function and synapse number [69]. Thus, by comparing differences between the RM proteome and $A\beta_{1-42}$-induced microglial proteome, new potential therapeutic targets can be identified that may promote an anti-AD intrinsic state in microglia.

It is important to note that there are some important limitations to our study. HEBSCs have many benefits, such as the presence of all tissue types. However, the brain slice cultures used lack several features found in vivo such as vascular supply, meninges, and the vascular

endothelium which play important roles in the secretion of Aβ from the brain as well as immune responses. There also is no involvement of the periphery which increasingly is being identified as important for AD progression. Further, the addition of $A\beta_{1-42}$ to the media is only an approximation of the process in vivo, in which Aβ is produced by neurons and encountered by local microglia. This raises the issue that our approach might result in homogenous microglia responses, since all microglia are exposed to equal concentrations of $A\beta_{1-42}$ rather than gradients of exposure seen in vivo. However, it is not clear that this is occurring since we see evidence of both protective and neurotoxic phenotypes. Nevertheless, our approach affords the advantage of making it easier to study the impact of soluble Aβ on microglia-related neuronal pathology, though it differs from the more spatial and proximity related exposures seen *in vivo.* Lastly, the HEBSC cultures are likely more similar to a young adult, but not aged brain. This may not necessarily be a severe limitation, since early Aβ pathology begins to emerge in midlife, decades prior to the emergence of symptoms [2].

In summary, we find that intrinsic microglial state governs the downstream consequences of $A\beta_{1-42}$ exposure. These intrinsic microglial states could be manipulated pharmacologically to reduce the adverse consequences of Aβ exposure.

Conclusions

Neuroimmune signaling including TRAIL and proinflammatory microglia promote excitotoxicity caused by soluble $A\beta_{1-42}$ oligomers. However, resting microglia restrain Aβ-induced toxicity, which is completely abolished by prior microglial repopulation. Proteomic analysis of repopulated and $A\beta_{1-42}$-exposed microglia identified targets for potential pharmacological intervention that could prevent Aβ-induced neurotoxicity.

Abbreviations

Aβ	Amyloid Beta
AD	Alzheimer's Disease
CSF1R	Colony Stimulating Factor 1 Receptor
DG	Dentate Gyrus
DR	Death Receptor
DREADD	Designer Receptor Exclusively Activated By Designer Drugs
FBS	Fetal Bovine Serum
FC	Fold Change
FDR	False Discovery Rate
GPCR	G Protein Coupled Receptor
HEBSC	Hippocampal Entorhinal Brain Slice Culture
hM4di	Gi DREADD
IPA	Ingenuity Pathway Analysis
LC-MS/MS	Lipid Chromatography Coupled with Mass Spectroscopy
MACS	Immunomagnetic Separation
MD	Microglial Depletion
PI	Propidium Iodide
RM	Repopulated Microglia
TLR	Toll–Like Receptor
TRAIL	TNF–Related Apoptosis–Inducing Ligand

Supplementary Information

The online version contains supplementary material available at https://doi.org/10.1186/s12974-024-03208-2.

Supplementary Material 1: Additional File 1

Supplementary Material 2: Supplemental Figure 1. Age-related increases in Aβ1-42 in 5xFAD. (A) Aβ1-42 increased in the dentate gyrus in both male and female 5xFAD from 3 to 6 months. 2-way ANOVA, Age effect, F1,23=106.0, p<0.0001. N=5-8/group. (B) Aβ1-42 in the CA1 of the hippocampus in male and female 5xFAD from 3 to 6 months. 2-way ANOVA, Age effect, F1,17=10.6, p=0.0047. N=5-7/group. **p<0.01, ****p<0.0001, Sidak's post-test

Supplementary Material 3: Supplemental Figure 2. Gi DREADD inhibition of microglia blunts A?-induced pro-inflammatory gene activation. HEBSCs were treated with AAV.CD68.hM4di (DREADD) or AAV.EGFP control viruses for 24 hours prior to treatment +/- Aβ1-42 +/- the DREADD ligand CNO (5μM). Aβ1-42 +/- CNO groups were combined due to the lack of a CNO effect. (A) Aβ1-42 increased gene expression of TNF? that was blunted by activation of Gi signaling with CNO. 1-way ANOVA, F4,12=8.1 treatment effect, p<0.01. (B) Aβ1–42 increased gene expression of Iba-1 that was blunted by Gi activation with CNO. 1-way ANOVA, F3,8=6.9 treatment effect. Sidak's multiple comparisons test. p<0.05. *p<0.05, **p<0.01, **p<0.001, ****p<0.0001. Each data point represents the average of replicates from 2 experiments. N=2-4/group

Supplementary Material 4: Supplemental Figure 4. Additional analyses from microglial proteomic assessment. Microglia were isolated from HEBSCs after microglial repopulation (RM) or treatment with Aβ1-42 for 24 hours and the microglial proteome assessed by LC-MS/MS. (A) Levels of microglia specific proteins that were enriched in isolated microglia from pooled control groups. (B) Complete IPA predicted network of RM vs control microglia. (C) Proteins increased in their abundance by A?1-42 that align with previous findings from Monasor et al. (D) Complete IPA predicted network of Aβ1-42 treated vs control microglia

Acknowledgements

We thank Jay Campbell for his support managing the animal colony. The senior author thanks God the Father for His guidance.

Author contributions

JZ performed culture experiments, analyzed data, and contributed to writing the manuscript. EM helped design and perform microglial isolation experiments and contributed to writing the manuscript. SG performed and analyzed immunohistochemistry. SL, AM, LH performed LC-MS/MS, analyzed the data, and edited the manuscript. RV designed and performed in vivo immunohistochemistry, analyzed the data, and contributed to writing the manuscript. LC designed the experiments, helped perform microglial isolation experiments, analyzed data, and wrote the majority of the manuscript. All authors read and approved the final manuscript.

Funding

This work was supported by grants awarded to L.C. from NIH (R01AA028924, K08AA024829), R.V. (R01AG072894, K01AA025713), and the UNC Bowles Center for Alcohol Studies. This research is based in part upon work conducted using the UNC Proteomics Core Facility, which is supported in part by NCI Center Core Support Grant (2P30CA016086-45) to the UNC Lineberger Comprehensive Cancer Center.

Data availability

The datasets generated and/or analyzed during the current study are in Additional File 1 and will be made available in the PRIDE repository at publication.

Declarations

Ethics approval and consent to participate

24–040, 24–096.

Consent for publication
Not applicable.

Competing interests
The authors declare no competing interests.

Author details
[1]Bowles Center for Alcohol Studies, University of North Carolina at Chapel Hill School of Medicine, Chapel Hill, NC 27599, USA
[2]Department of Psychiatry, University of North Carolina at Chapel Hill School of Medicine, Chapel Hill, NC 27599, USA
[3]Department of Pharmacology, UNC Proteomics Core, University of North Carolina at Chapel Hill School of Medicine, Chapel Hill, NC 27599, USA
[4]Department of Pharmacology, University of North Carolina at Chapel Hill School of Medicine, Chapel Hill, NC 27599, USA

Received: 28 June 2024 / Accepted: 26 August 2024
Published online: 01 September 2024

References

1. Collaborators GBDDF. Estimation of the global prevalence of dementia in 2019 and forecasted prevalence in 2050: an analysis for the global burden of Disease Study 2019. Lancet Public Health. 2022;7(2):e105–25.
2. Long JM, Holtzman DM. Alzheimer Disease: an update on pathobiology and treatment strategies. Cell. 2019;179(2):312–39.
3. Blomeke L, Rehn F, Kraemer-Schulien V, Kutzsche J, Pils M, Bujnicki T, et al. Abeta oligomers peak in early stages of Alzheimer's disease preceding tau pathology. Alzheimers Dement (Amst). 2024;16(2):e12589.
4. Haass C, Kaether C, Thinakaran G, Sisodia S. Trafficking and proteolytic processing of APP. Cold Spring Harb Perspect Med. 2012;2(5):a006270.
5. Zott B, Simon MM, Hong W, Unger F, Chen-Engerer HJ, Frosch MP, et al. A vicious cycle of beta amyloid-dependent neuronal hyperactivation. Science. 2019;365(6453):559–65.
6. Resende R, Ferreiro E, Pereira C, Resende de Oliveira C. Neurotoxic effect of oligomeric and fibrillar species of amyloid-beta peptide 1–42: involvement of endoplasmic reticulum calcium release in oligomer-induced cell death. Neuroscience. 2008;155(3):725–37.
7. Cizas P, Budvytyte R, Morkuniene R, Moldovan R, Broccio M, Losche M, et al. Size-dependent neurotoxicity of beta-amyloid oligomers. Arch Biochem Biophys. 2010;496(2):84–92.
8. Yang T, Li S, Xu H, Walsh DM, Selkoe DJ. Large soluble oligomers of amyloid beta-protein from Alzheimer Brain are far less neuroactive than the smaller oligomers to which they dissociate. J Neuroscience: Official J Soc Neurosci. 2017;37(1):152–63.
9. Chapman PF, White GL, Jones MW, Cooper-Blacketer D, Marshall VJ, Irizarry M, et al. Impaired synaptic plasticity and learning in aged amyloid precursor protein transgenic mice. Nat Neurosci. 1999;2(3):271–6.
10. Walsh DM, Klyubin I, Fadeeva JV, Cullen WK, Anwyl R, Wolfe MS, et al. Naturally secreted oligomers of amyloid beta protein potently inhibit hippocampal long-term potentiation in vivo. Nature. 2002;416(6880):535–9.
11. Shankar GM, Bloodgood BL, Townsend M, Walsh DM, Selkoe DJ, Sabatini BL. Natural oligomers of the Alzheimer amyloid-beta protein induce reversible synapse loss by modulating an NMDA-type glutamate receptor-dependent signaling pathway. J Neuroscience: Official J Soc Neurosci. 2007;27(11):2866–75.
12. Busche MA, Eichhoff G, Adelsberger H, Abramowski D, Wiederhold KH, Haass C, et al. Clusters of hyperactive neurons near amyloid plaques in a mouse model of Alzheimer's disease. Science. 2008;321(5896):1686–9.
13. Palop JJ, Mucke L. Network abnormalities and interneuron dysfunction in Alzheimer disease. Nat Rev Neurosci. 2016;17(12):777–92.
14. Davis DG, Schmitt FA, Wekstein DR, Markesbery WR. Alzheimer neuropathologic alterations in aged cognitively normal subjects. J Neuropathol Exp Neurol. 1999;58(4):376–88.
15. Fagan AM, Mintun MA, Shah AR, Aldea P, Roe CM, Mach RH, et al. Cerebrospinal fluid tau and ptau(181) increase with cortical amyloid deposition in cognitively normal individuals: implications for future clinical trials of Alzheimer's disease. EMBO Mol Med. 2009;1(8–9):371–80.
16. Chetelat G, La Joie R, Villain N, Perrotin A, de La Sayette V, Eustache F, et al. Amyloid imaging in cognitively normal individuals, at-risk populations and preclinical Alzheimer's disease. Neuroimage Clin. 2013;2:356–65.
17. Jack CR Jr., Wiste HJ, Schwarz CG, Lowe VJ, Senjem ML, Vemuri P, et al. Longitudinal tau PET in ageing and Alzheimer's disease. Brain. 2018;141(5):1517–28.
18. Schultz SA, Gordon BA, Mishra S, Su Y, Perrin RJ, Cairns NJ, et al. Widespread distribution of tauopathy in preclinical Alzheimer's disease. Neurobiol Aging. 2018;72:177–85.
19. Zhang B, Gaiteri C, Bodea LG, Wang Z, McElwee J, Podtelezhnikov AA, et al. Integrated systems approach identifies genetic nodes and networks in late-onset Alzheimer's disease. Cell. 2013;153(3):707–20.
20. Heneka MT, Carson MJ, El Khoury J, Landreth GE, Brosseron F, Feinstein DL, et al. Neuroinflammation in Alzheimer's disease. Lancet Neurol. 2015;14(4):388–405.
21. Jack CR Jr., Bennett DA, Blennow K, Carrillo MC, Dunn B, Haeberlein SB, et al. NIA-AA Research Framework: toward a biological definition of Alzheimer's disease. Alzheimer's Dement J Alzheimer's Assoc. 2018;14(4):535–62.
22. Dani M, Wood M, Mizoguchi R, Fan Z, Walker Z, Morgan R, et al. Microglial activation correlates in vivo with both tau and amyloid in Alzheimer's disease. Brain. 2018;141(9):2740–54.
23. Lee DC, Rizer J, Selenica ML, Reid P, Kraft C, Johnson A, et al. LPS- induced inflammation exacerbates phospho-tau pathology in rTg4510 mice. J Neuroinflamm. 2010;7:56.
24. Sheng JG, Bora SH, Xu G, Borchelt DR, Price DL, Koliatsos VE. Lipopolysaccharide-induced-neuroinflammation increases intracellular accumulation of amyloid precursor protein and amyloid beta peptide in APPswe transgenic mice. Neurobiol Dis. 2003;14(1):133–45.
25. Barnett AM, David E, Rohlman AR, Nikolova VD, Moy SS, Vetreno R, et al. Adolescent binge alcohol enhances early Alzheimer's Disease Pathology in Adulthood through Proinflammatory Neuroimmune activation. Front Pharmacol. 2022;13:884170.
26. Henry CM, Martin SJ. Caspase-8 acts in a non-enzymatic role as a Scaffold for Assembly of a pro-inflammatory FADDosome complex upon TRAIL stimulation. Mol Cell. 2017;65(4):715–29. e5.
27. Burgaletto C, Munafo A, Di Benedetto G, De Francisci C, Caraci F, Di Mauro R, et al. The immune system on the TRAIL of Alzheimer's disease. J Neuroinflamm. 2020;17(1):298.
28. Uberti D, Ferrari-Toninelli G, Bonini SA, Sarnico I, Benarese M, Pizzi M, et al. Blockade of the tumor necrosis factor-related apoptosis inducing ligand death receptor DR5 prevents beta-amyloid neurotoxicity. Neuropsychopharmacology: Official Publication Am Coll Neuropsychopharmacol. 2007;32(4):872–80.
29. Uberti D, Cantarella G, Facchetti F, Cafici A, Grasso G, Bernardini R, et al. TRAIL is expressed in the brain cells of Alzheimer's disease patients. NeuroReport. 2004;15(4):579–81.
30. Cantarella G, Uberti D, Carsana T, Lombardo G, Bernardini R, Memo M. Neutralization of TRAIL death pathway protects human neuronal cell line from beta-amyloid toxicity. Cell Death Differ. 2003;10(1):134–41.
31. Burgaletto C, Platania CBM, Di Benedetto G, Munafo A, Giurdanella G, Federico C, et al. Targeting the miRNA-155/TNFSF10 network restrains inflammatory response in the retina in a mouse model of Alzheimer's disease. Cell Death Dis. 2021;12(10):905.
32. Qin L, Zou J, Barnett A, Vetreno RP, Crews FT, Coleman LG. TRAIL mediates neuronal death in AUD: a link between Neuroinflammation and Neurodegeneration. Int J Mol Sci. 2021;22(5):2547.
33. Coleman LG Jr., Zou J, Crews FT. Microglial-derived miRNA let-7 and HMGB1 contribute to ethanol-induced neurotoxicity via TLR7. J Neuroinflamm. 2017;14(1):22.
34. Leng F, Edison P. Neuroinflammation and microglial activation in Alzheimer disease: where do we go from here? Nat Rev Neurol. 2021;17(3):157–72.
35. Keren-Shaul H, Spinrad A, Weiner A, Matcovitch-Natan O, Dvir-Szternfeld R, Ulland TK, et al. A Unique Microglia Type Associated with Restricting Development of Alzheimer's Disease. Cell. 2017;169(7):1276–e9017.
36. Ennerfelt H, Frost EL, Shapiro DA, Holliday C, Zengeler KE, Voithofer G, et al. SYK coordinates neuroprotective microglial responses in neurodegenerative disease. Cell. 2022;185(22):4135–52. e22.
37. Wang S, Sudan R, Peng V, Zhou Y, Du S, Yuede CM, et al. TREM2 drives microglia response to amyloid-beta via SYK-dependent and -independent pathways. Cell. 2022;185(22):4153–e6919.
38. Del Bo R, Angeretti N, Lucca E, De Simoni MG, Forloni G. Reciprocal control of inflammatory cytokines, IL-1 and IL-6, and beta-amyloid production in cultures. Neurosci Lett. 1995;188(1):70–4.
39. Solito E, Sastre M. Microglia function in Alzheimer's disease. Front Pharmacol. 2012;3:14.

40. Luciunaite A, McManus RM, Jankunec M, Racz I, Dansokho C, Dalgediene I, et al. Soluble abeta oligomers and protofibrils induce NLRP3 inflammasome activation in microglia. J Neurochem. 2020;155(6):650–61.
41. Dalgediene I, Lasickiene R, Budvytyte R, Valincius G, Morkuniene R, Borutaite V, et al. Immunogenic properties of amyloid beta oligomers. J Biomed Sci. 2013;20(1):10.
42. Walter S, Letiembre M, Liu Y, Heine H, Penke B, Hao W, et al. Role of the toll-like receptor 4 in neuroinflammation in Alzheimer's disease. Cell Physiol Biochem. 2007;20(6):947–56.
43. Jin JJ, Kim HD, Maxwell JA, Li L, Fukuchi K. Toll-like receptor 4-dependent upregulation of cytokines in a transgenic mouse model of Alzheimer's disease. J Neuroinflamm. 2008;5:23.
44. Song M, Jin J, Lim JE, Kou J, Pattanayak A, Rehman JA, et al. TLR4 mutation reduces microglial activation, increases Abeta deposits and exacerbates cognitive deficits in a mouse model of Alzheimer's disease. J Neuroinflamm. 2011;8:92.
45. Hsiao CC, Sankowski R, Prinz M, Smolders J, Huitinga I, Hamann J. GPCRomics of homeostatic and Disease-Associated Human Microglia. Front Immunol. 2021;12:674189.
46. Zou J, Walter TJ, Barnett A, Rohlman A, Crews FT, Coleman LG. Ethanol induces secretion of Proinflammatory Extracellular vesicles that inhibit adult hippocampal neurogenesis through G9a/GLP-Epigenetic signaling. Front Immunol. 2022;13.
47. Coleman LG Jr., Zou J, Crews FT. Microglial depletion and repopulation in brain slice culture normalizes sensitized proinflammatory signaling. J Neuroinflamm. 2020;17(1):27.
48. Grace PM, Wang X, Strand KA, Baratta MV, Zhang Y, Galer EL, et al. DREADDed microglia in pain: implications for spinal inflammatory signaling in male rats. Exp Neurol. 2018;304:125–31.
49. Elmore MRP, Hohsfield LA, Kramar EA, Soreq L, Lee RJ, Pham ST, et al. Replacement of microglia in the aged brain reverses cognitive, synaptic, and neuronal deficits in mice. Aging Cell. 2018;17(6):e12832.
50. Humpel C. Organotypic brain slice cultures: a review. Neuroscience. 2015;305:86–98.
51. Stoppini L, Buchs PA, Muller D. A simple method for organotypic cultures of nervous tissue. J Neurosci Methods. 1991;37(2):173–82.
52. Nagerl UV, Willig KI, Hein B, Hell SW, Bonhoeffer T. Live-cell imaging of dendritic spines by STED microscopy. Proc Natl Acad Sci USA. 2008;105(48):18982–7.
53. Bonhoeffer T, Yuste R. Spine motility. Phenomenology, mechanisms, and function. Neuron. 2002;35(6):1019–27.
54. Hasegawa S, Sakuragi S, Tominaga-Yoshino K, Ogura A. Dendritic spine dynamics leading to spine elimination after repeated inductions of LTD. Sci Rep. 2015;5:7707.
55. Verkuyl JM, Matus A. Time-lapse imaging of dendritic spines in vitro. Nat Protoc. 2006;1(5):2399–405.
56. Hoppe JB, Haag M, Whalley BJ, Salbego CG, Cimarosti H. Curcumin protects organotypic hippocampal slice cultures from Abeta1-42-induced synaptic toxicity. Toxicol Vitro. 2013;27(8):2325–30.
57. Zou J, Crews F. CREB and NF-kappaB transcription factors regulate sensitivity to excitotoxic and oxidative stress induced neuronal cell death. Cell Mol Neurobiol. 2006;26(4–6):385–405.
58. Noraberg J, Kristensen BW, Zimmer J. Markers for neuronal degeneration in organotypic slice cultures. Brain Res Brain Res Protoc. 1999;3(3):278–90.
59. Zimmer J, Kristensen BW, Jakobsen B, Noraberg J. Excitatory amino acid neurotoxicity and modulation of glutamate receptor expression in organotypic brain slice cultures. Amino Acids. 2000;19(1):7–21.
60. Grace PM, Strand KA, Galer EL, Urban DJ, Wang X, Baratta MV, et al. Morphine paradoxically prolongs neuropathic pain in rats by amplifying spinal NLRP3 inflammasome activation. Proc Natl Acad Sci USA. 2016;113(24):E3441–50.
61. Bordt EA, Block CL, Petrozziello T, Sadri-Vakili G, Smith CJ, Edlow AG et al. Isolation of Microglia from Mouse or Human tissue. STAR Protoc. 2020;1(1).
62. Tyanova S, Temu T, Sinitcyn P, Carlson A, Hein MY, Geiger T, et al. The Perseus computational platform for comprehensive analysis of (prote)omics data. Nat Methods. 2016;13(9):731–40.
63. Zou J, Crews FT. Glutamate/NMDA excitotoxicity and HMGB1/TLR4 neuroimmune toxicity converge as components of neurodegenration. AIMS Mol Sci. 2015;2(2):77–100.
64. Zou J, Crews FT. Glutamate/NMDA excitotoxicity and HMGB1/TLR4 neuroimmune toxicity converge as components of neurodegeneration. Aims Mol Sci. 2015;2(2):77–100.
65. Crews FT, Qin L, Sheedy D, Vetreno RP, Zou J. High mobility group box 1/Toll-like receptor danger signaling increases brain neuroimmune activation in alcohol dependence. Biol Psychiatry. 2013;73(7):602–12.
66. Maes ME, Colombo G, Schulz R, Siegert S. Targeting microglia with lentivirus and AAV: recent advances and remaining challenges. Neurosci Lett. 2019;707:134310.
67. Crews FT, Zou J, Coleman LG. Jr. Extracellular microvesicles promote microglia-mediated pro-inflammatory responses to ethanol. J Neurosci Res. 2021;99(8):1940–56.
68. Barnett AM, Crews FT, Coleman LG. Microglial depletion and repopulation: a new era of regenerative medicine? Neural Regen Res. 2021;16(6):1204–5.
69. Wang W, Li Y, Ma F, Sheng X, Chen K, Zhuo R, et al. Microglial repopulation reverses cognitive and synaptic deficits in an Alzheimer's disease model by restoring BDNF signaling. Brain Behav Immun. 2023;113:275–88.
70. Sebastian Monasor L, Muller SA, Colombo AV, Tanrioever G, Konig J, Roth S et al. Fibrillar abeta triggers microglial proteome alterations and dysfunction in Alzheimer mouse models. Elife. 2020;9.
71. Wilson NS, Dixit V, Ashkenazi A. Death receptor signal transducers: nodes of coordination in immune signaling networks. Nat Immunol. 2009;10(4):348–55.
72. Cantarella G, Di Benedetto G, Puzzo D, Privitera L, Loreto C, Saccone S, et al. Neutralization of TNFSF10 ameliorates functional outcome in a murine model of Alzheimer's disease. Brain. 2015;138(Pt 1):203–16.
73. Di Benedetto G, Burgaletto C, Carta AR, Saccone S, Lempereur L, Mulas G, et al. Beneficial effects of curtailing immune susceptibility in an Alzheimer's disease model. J Neuroinflamm. 2019;16(1):166.
74. Cui M, Wang L, Liang X, Ma X, Liu Y, Yang M, et al. Blocking TRAIL-DR5 signaling with soluble DR5 reduces delayed neuronal damage after transient global cerebral ischemia. Neurobiol Dis. 2010;39(2):138–47.
75. Croft M, Siegel RM, Beyond TNF. TNF superfamily cytokines as targets for the treatment of rheumatic diseases. Nat Rev Rheumatol. 2017;13(4):217–33.
76. Mahmood Z, Shukla Y. Death receptors: targets for cancer therapy. Exp Cell Res. 2010;316(6):887–99.
77. Safa AR. c-FLIP, a master anti-apoptotic regulator. Exp Oncol. 2012;34(3):176–84.
78. Twohig JP, Cuff SM, Yong AA, Wang EC. The role of tumor necrosis factor receptor superfamily members in mammalian brain development, function and homeostasis. Rev Neurosci. 2011;22(5):509–33.
79. Niu Y, Li Y, Zang J, Huang H, Deng J, Cui Z, et al. Death receptor 5 and neuroproliferation. Cell Mol Neurobiol. 2012;32(2):255–65.
80. Lawrimore CJ, Coleman LG, Crews FT. Ethanol induces interferon expression in neurons via TRAIL: role of astrocyte-to-neuron signaling. Psychopharmacology. 2019.
81. Kichev A, Rousset CI, Baburamani AA, Levison SW, Wood TL, Gressens P, et al. Tumor necrosis factor-related apoptosis-inducing ligand (TRAIL) signaling and cell death in the immature central nervous system after hypoxia-ischemia and inflammation. J Biol Chem. 2014;289(13):9430–9.
82. Oldenhuis CN, Stegehuis JH, Walenkamp AM, de Jong S, de Vries EG. Targeting TRAIL death receptors. Curr Opin Pharmacol. 2008;8(4):433–9.
83. Di Cristofano F, George A, Tajiknia V, Ghandali M, Wu L, Zhang Y, et al. Therapeutic targeting of TRAIL death receptors. Biochem Soc Trans. 2023;51(1):57–70.
84. Tisato V, Gonelli A, Voltan R, Secchiero P, Zauli G. Clinical perspectives of TRAIL: insights into central nervous system disorders. Cell Mol Life Sci. 2016;73(10):2017–27.
85. Moreno-Gonzalez I, Baglietto-Vargas D, Sanchez-Varo R, Jimenez S, Trujillo-Estrada L, Sanchez-Mejias E, et al. Extracellular amyloid-beta and cytotoxic glial activation induce significant entorhinal neuron loss in young PS1(M146L)/APP(751SL) mice. J Alzheimer's Disease: JAD. 2009;18(4):755–76.
86. Eimer WA, Vassar R. Neuron loss in the 5XFAD mouse model of Alzheimer's disease correlates with intraneuronal Abeta42 accumulation and Caspase-3 activation. Mol Neurodegeneration. 2013;8:2.
87. Ross RD, Shah RC, Leurgans S, Bottiglieri T, Wilson RS, Sumner DR. Circulating Dkk1 and TRAIL are Associated with Cognitive decline in Community-Dwelling, older adults with cognitive concerns. J Gerontol Biol Sci Med Sci. 2018;73(12):1688–94.
88. Tian X, Zhao Z, Zhao J, Su D, He B, Shi C, et al. Transcriptomic analysis to identify genes associated with hypothalamus vulnerability in aging mice with cognitive decline. Behav Brain Res. 2024;465:114943.
89. Ximerakis M, Lipnick SL, Innes BT, Simmons SK, Adiconis X, Dionne D, et al. Single-cell transcriptomic profiling of the aging mouse brain. Nat Neurosci. 2019;22(10):1696–708.

90. Lopes KP, Snijders GJL, Humphrey J, Allan A, Sneeboer MAM, Navarro E, et al. Genetic analysis of the human microglial transcriptome across brain regions, aging and disease pathologies. Nat Genet. 2022;54(1):4–17.
91. Efthymiou AG, Goate AM. Late onset Alzheimer's disease genetics implicates microglial pathways in disease risk. Mol Neurodegeneration. 2017;12(1):43.
92. Sims R, van der Lee SJ, Naj AC, Bellenguez C, Badarinarayan N, Jakobsdottir J, et al. Rare coding variants in PLCG2, ABI3, and TREM2 implicate microglial-mediated innate immunity in Alzheimer's disease. Nat Genet. 2017;49(9):1373–84.
93. Jonsson T, Stefansson H, Steinberg S, Jonsdottir I, Jonsson PV, Snaedal J, et al. Variant of TREM2 associated with the risk of Alzheimer's disease. N Engl J Med. 2013;368(2):107–16.
94. Balducci C, Frasca A, Zotti M, La Vitola P, Mhillaj E, Grigoli E, et al. Toll-like receptor 4-dependent glial cell activation mediates the impairment in memory establishment induced by beta-amyloid oligomers in an acute mouse model of Alzheimer's disease. Brain Behav Immun. 2017;60:188–97.
95. Rosenberger K, Derkow K, Dembny P, Kruger C, Schott E, Lehnardt S. The impact of single and pairwise toll-like receptor activation on neuroinflammation and neurodegeneration. J Neuroinflamm. 2014;11:166.
96. Rajendran L, Paolicelli RC. Microglia-mediated synapse loss in Alzheimer's Disease. J Neuroscience: Official J Soc Neurosci. 2018;38(12):2911–9.
97. Liddelow SA, Guttenplan KA, Clarke LE, Bennett FC, Bohlen CJ, Schirmer L, et al. Neurotoxic reactive astrocytes are induced by activated microglia. Nature. 2017;541(7638):481–7.
98. Salvadores N, Moreno-Gonzalez I, Gamez N, Quiroz G, Vegas-Gomez L, Escandon M, et al. Abeta oligomers trigger necroptosis-mediated neurodegeneration via microglia activation in Alzheimer's disease. Acta Neuropathol Commun. 2022;10(1):31.
99. Spangenberg E, Severson PL, Hohsfield LA, Crapser J, Zhang J, Burton EA, et al. Sustained microglial depletion with CSF1R inhibitor impairs parenchymal plaque development in an Alzheimer's disease model. Nat Commun. 2019;10(1):3758.
100. Hong S, Beja-Glasser VF, Nfonoyim BM, Frouin A, Li S, Ramakrishnan S, et al. Complement and microglia mediate early synapse loss in Alzheimer mouse models. Science. 2016;352(6286):712–6.
101. Wang C, Fan L, Khawaja RR, Liu B, Zhan L, Kodama L, et al. Microglial NF-kappaB drives tau spreading and toxicity in a mouse model of tauopathy. Nat Commun. 2022;13(1):1969.
102. Spangenberg EE, Lee RJ, Najafi AR, Rice RA, Elmore MR, Blurton-Jones M, et al. Eliminating microglia in Alzheimer's mice prevents neuronal loss without modulating amyloid-beta pathology. Brain. 2016;139(Pt 4):1265–81.
103. Parusel S, Yi MH, Hunt CL, Wu LJ. Chemogenetic and optogenetic manipulations of Microglia in Chronic Pain. Neurosci Bull. 2023;39(3):368–78.
104. Richter M, Vidovic N, Biber K, Dolga A, Culmsee C, Dodel R. The neuroprotective role of microglial cells against amyloid beta-mediated toxicity in organotypic hippocampal slice cultures. Brain Pathol. 2020;30(3):589–602.
105. Diaz-Aparicio I, Paris I, Sierra-Torre V, Plaza-Zabala A, Rodriguez-Iglesias N, Marquez-Ropero M, et al. Microglia actively remodel adult hippocampal neurogenesis through the phagocytosis secretome. J Neuroscience: Official J Soc Neurosci. 2020;40(7):1453–82.
106. Almasan A, Ashkenazi A. Apo2L/TRAIL: apoptosis signaling, biology, and potential for cancer therapy. Cytokine Growth Factor Rev. 2003;14(3–4):337–48.
107. Huang Y, Walstrom A, Zhang L, Zhao Y, Cui M, Ye L, et al. Type I interferons and interferon regulatory factors regulate TNF-related apoptosis-inducing ligand (TRAIL) in HIV-1-infected macrophages. PLoS ONE. 2009;4(4):e5397.
108. Peteranderl C, Herold S. The impact of the Interferon/TNF-Related apoptosis-inducing ligand Signaling Axis on Disease Progression in respiratory viral infection and Beyond. Front Immunol. 2017;8:313.
109. Sato K, Hida S, Takayanagi H, Yokochi T, Kayagaki N, Takeda K, et al. Antiviral response by natural killer cells through TRAIL gene induction by IFN-alpha/beta. Eur J Immunol. 2001;31(11):3138–46.
110. Roy ER, Wang B, Wan YW, Chiu G, Cole A, Yin Z, et al. Type I interferon response drives neuroinflammation and synapse loss in Alzheimer disease. J Clin Investig. 2020;130(4):1912–30.
111. Roy ER, Chiu G, Li S, Propson NE, Kanchi R, Wang B, et al. Concerted type I interferon signaling in microglia and neural cells promotes memory impairment associated with amyloid beta plaques. Immunity. 2022;55(5):879–94.e6.
112. Holtman IR, Raj DD, Miller JA, Schaafsma W, Yin Z, Brouwer N, et al. Induction of a common microglia gene expression signature by aging and neurodegenerative conditions: a co-expression meta-analysis. Acta Neuropathol Commun. 2015;3:31.
113. Galatro TF, Holtman IR, Lerario AM, Vainchtein ID, Brouwer N, Sola PR, et al. Transcriptomic analysis of purified human cortical microglia reveals age-associated changes. Nat Neurosci. 2017;20(8):1162–71.
114. Prater KE, Green KJ, Mamde S, Sun W, Cochoit A, Smith CL, et al. Human microglia show unique transcriptional changes in Alzheimer's disease. Nat Aging. 2023;3(7):894–907.
115. Puthia M, Ambite I, Cafaro C, Butler D, Huang Y, Lutay N, et al. IRF7 inhibition prevents destructive innate immunity-A target for nonantibiotic therapy of bacterial infections. Sci Transl Med. 2016;8(336):336ra59.
116. Lehmann SM, Kruger C, Park B, Derkow K, Rosenberger K, Baumgart J, et al. An unconventional role for miRNA: let-7 activates toll-like receptor 7 and causes neurodegeneration. Nat Neurosci. 2012;15(6):827–35.
117. Lehmann SM, Rosenberger K, Kruger C, Habbel P, Derkow K, Kaul D, et al. Extracellularly delivered single-stranded viral RNA causes neurodegeneration dependent on TLR7. J Immunol. 2012;189(3):1448–58.
118. Port A, Shaw JV, Klopp-Schulze L, Bytyqi A, Vetter C, Hussey E, et al. Phase 1 study in healthy participants of the safety, pharmacokinetics, and pharmacodynamics of enpatoran (M5049), a dual antagonist of toll-like receptors 7 and 8. Pharmacol Res Perspect. 2021;9(5):e00842.
119. Flowers A, Bell-Temin H, Jalloh A, Stevens SM Jr., Bickford PC. Proteomic anaysis of aged microglia: shifts in transcription, bioenergetics, and nutrient response. J Neuroinflamm. 2017;14(1):96.
120. Shi Q, Chang C, Saliba A, Bhat MA. Microglial mTOR activation upregulates Trem2 and enhances beta-amyloid plaque clearance in the 5XFAD Alzheimer's Disease Model. J Neuroscience: Official J Soc Neurosci. 2022;42(27):5294–313.
121. Townsend KP, Town T, Mori T, Lue LF, Shytle D, Sanberg PR, et al. CD40 signaling regulates innate and adaptive activation of microglia in response to amyloid beta-peptide. Eur J Immunol. 2005;35(3):901–10.

Publisher's note